**Numerical assessment and evaluation of a stream modification strategy to address sediment aggradation issues at the Dean Road bridge in Dale County, Alabama**

by

Wenjun Song

A thesis submitted to the Graduate Faculty of
Auburn University
in partial fulfillment of the
requirements for the Degree of
Master of Science

Auburn, Alabama
May 4, 2019

Keywords: Numerical models, River hydraulics, Sediment aggradation, Bridges



Approved by

Jose G. Vasconcelos, Chair, Associate Professor of Civil Engineering
Xing Fang, Arthur H. Feagin Chair Professor of Civil Engineering
J. Brian Anderson, Associate Professor of Civil Engineering

Abstract

Severe aggradation in bridge structures is a serious issue since it may lead to overtopping episodes during peak flows or increased risk of serious structural damage. Aggradation processes may be caused by changes in watershed land use or clear-cutting near streams among others causes. In order to predict aggradation and degradation in the river, filed data were collected and hydrologic and hydraulic models are built. Field monitoring data, such as rainfall, water depth, water velocity and sediment concentration were collected through sensors and water samples. These field measurements were used in the model as inputs to enable building and calibration of the model. River modeling tools, such as HEC-RAS and SRH-2D, are useful in computing characteristics of stream flow, such as velocities and stages, if aggradation processes take place. While the field monitoring data (rainfall data) were used as the model input of hydrologic model (HEC-HMS), the discharge of the hydrologic model is used as the input of the hydraulic model. These models can also be used to assess proposed changes in the stream characteristics to minimize aggradation issues, including stream modification with the objective of increasing flow velocities near the roadway-stream crossing. This work presents results of using HEC-RAS 5 and SRH-2D to estimate the impacts of aggradation and proposed geometric changes in a stream in Southeast Alabama. One specific point (under the bridge) with monitoring data was selected from the two models and the results are compared. Results indicate important impacts of geometric details in the stream flow characteristics, and indeed point to the benefits of using a 2D modeling approaches to evaluate the impacts of stream modifications to reduce aggradation issues.

Table of Contents

List of Figures

List of Tables

List of Abbreviations

List of symbols (Latin Letters)

| | |
|---|---|
| $A$ | Cross sectional area of the open channel flow |
| $E$ | Specific energy |
| $f$ | Coriolis parameter |
| $G$ | Charge per unit width |
| $g$ | Acceleration of gravity |
| $H$ | Water elevation |
| $h$ | Water depth |
| $K_1$ | Linear diffusion coefficient |
| $l_k$ | Length of the edge |
| $n$ | Manning roughness number |
| $n_k$ | Unit vector at face k in the cell |
| $P$ | Area of the cell neglecting the change of the slope |
| $Q$ | Volumetric flow rate |
| $q$ | Source/sink flux |
| $S$ | Boundary of cell |

$S_0$ Bed slope

$S_f$ Frictional slope

$u$ Velocity along x direction

$V$ 2D Velocity vector

$v$ Velocity along y direction

$V_k$ Average velocity at face k in the cell

$v_t$ Eddy viscosity coefficient

$Z$ Change in bed elevation

$z$ Bed elevation

List of symbols (Greek Letters)

$\alpha$ Dimensionless factor within sediment aggradation modeling

$\beta$ Dimensionless factor used in diffusive wave equation derivation

$\Gamma$ diffusivity factor

$\lambda$ bed material porosity

$\nabla$ partial derivative operator given by $\nabla = (\frac{\partial}{\partial x}, \frac{\partial}{\partial y})$

$\Omega$ 3D volume occupied by the fluid

$\phi$ any dependent variable

$\varphi$ latitude

List of Abbreviations

ALDOT - Alabama Department of Transportation

FESWMS - Finite Element Surface Water Modeling System

FHWA - Federal Highway Administration

HEC-HMS - Hydrologic Engineering Center Hydrologic Modeling System

HEC-RAS - Hydrologic Engineering Center River Analysis System

NOAA - National Oceanic and Atmospheric Administration

SRH-2D - Sedimentation and River Hydraulics - Two-Dimensional model

USBR - United States Bureau of Reclamation

USGU HUC - United States Geological Survey Hydrologic Unit Code

# Chapter 1

# Introduction

Changes in land uses caused by human activities in watersheds are known to create impacts to natural systems, including streams, rivers and other water bodies. Among the various impacts, of particular relevance are those related to watershed and stream bank erosion. This issue is recognized in technical literature, and Castro and Reckendorf (1995) presented a summary of the various impacts of sediments to various water bodies, both in terms of water quality and quantity. The authors state that sediment impacts are complex, multi-fold, and have cumulative effects in streams and rivers that are difficult to reproduce in laboratory conditions.

Human activities that are linked to severe sediment loadings include construction sites (Harbor, 1999), clear-cutting of forested areas (Brown and Krygier, 1971), and poorly managed agricultural practices. When these activities occur close to water bodies, the potential for these impacts increase. Other factors may trigger gradual increase in sediments in water bodies, such as short-term climatic events, in-stream alterations or changes in land management. Impacts in water quality and quantities in streams are immediate to aquatic species such as fish and macroinvertebrates.

Changes in river/stream hydrology, sediment generation and sediment transport can also create severe impacts to man-made structures such as bridges and culverts. For instance, watershed urbanization may contribute to larger peak runoff flows and volumes, which in turn may lead to increase in stream flow velocities, stream bank erosion, stream bank failure, and scouring. Activities such as forest clear-cutting can generate a significant increase in sediment loadings that can enter streams and lead to aggradation. Poor agricultural practices can also be a source of sediments to streams, which in turn may also lead to aggradation. Aggradation can be defined as the accumulation of sediments in in-stream structures that can impact and reduce the stream conveyance characteristics.

According to the Federal Highway Administration (FHWA), there are more than 600,000 bridges in the National Bridge Inventory (NBI) that are built over streams (FHWA, 2018). There are a large proportion of these bridges built over alluvial streams that are continually adjusting their beds and banks. Stream instability includes aggradation, degradation, bank erosion, and lateral channel shift during the useful life of the bridge. FHWA has released a series of publications focusing in river hydraulics through its Hydraulic Engineering Circular (HEC) series. Among these included HEC-18 (Arneson et al., 2012), HEC-20 (Lagasse et al., 2012), HEC-23 (Lagasse et al., 2009), and HDS-6 (Richardson et al., 2001). Most of these documents provide some guidance on stream instability, but the primary focus of these documents is scour at bridge sites, and limited information is given about stream aggradation and its countermeasures.

Johnson et al. (2001) reported that aggradation at bridges occurs in the arid regions, Midwest states, such as Iowa and Tennessee, and in a number of mid-Atlantic states, such as Pennsylvania, New York, and West Virginia. For example, in 1972, Hurricane Agnes destabilized large portions of the channels in the Bentley Creek watershed, causing a significant increase in bank erosion and subsequent movement of sediment (non-cohesive sand, gravel, cobbles, and boulders) through the channels. However, to this date, there is limited guidance to other States Departments of Transportation as to how to address specific issues related to aggradation in streams.

## 1.1 Problem statement

A severe aggradation process is ongoing in Soapstone Branch, located in Dale County, Alabama, which is a tributary of the Little Choctawhatchee River (USGS HUC 0314020105). As shown in Figure 1.1, the small stream and its watershed are near the southeast edge of Dale County. Figure 1.2 presents the aggradation condition at the Dean Road Bridge (BIN 12930) where Dean Road (Dale Co. Road 560) intercepts Soapstone Branch.

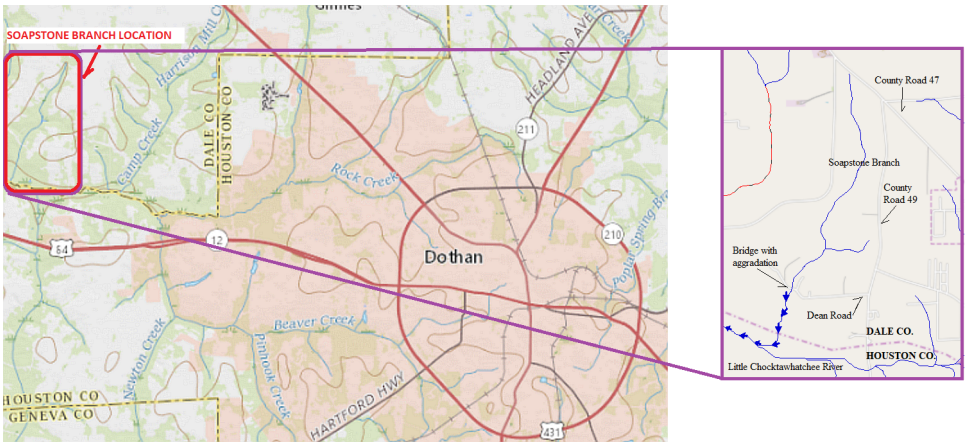


Figure 1.1: Location of Soapstone Branch and Dean Road within Dale County, AL

Figure 1.2: Aggradation in Soapstone Branch under Dean Road Bridge (Field visit on 8/11/2015)

According to the Alabama Department of Transportation (ALDOT), Dale County has diagnosed this aggradation problem in the bridge crossing in 2013, and by April 2014 there was only 2 inches of clearance beneath the bridge deck. Sediment excavation at the bridge vicinity was performed in early 2015, however by August 11, 2015 sediment had almost blocked the bridge, limiting again its flow conveyance. As a result of this aggradation, the bridge has the

potential of overtopping when moderate rain events occur in the Soapstone Branch watershed, as it is illustrated in Figure 1.3.

Figure 1.3: Overtopping at Dean Road Bridge during a storm event of 02/03/2016

Several potential factors could be playing a role in the issue of sediment blockage at the Dean Road Bridge. As is indicated in Figure 1.4, rainfall in the region has fluctuated significantly in recent years, with peaks well above the long-term average. Severe rain events can create episodes of large surface runoff and exacerbate issues of sediment generation within watershed, stream bank failure, and stream bank erosion. These factors can have an impact in the amount of sediment that is generated in the watershed and conveyed to the Dean Road Bridge. This was studied in detail by Tamang (2017) and Tamang et al. (2018).

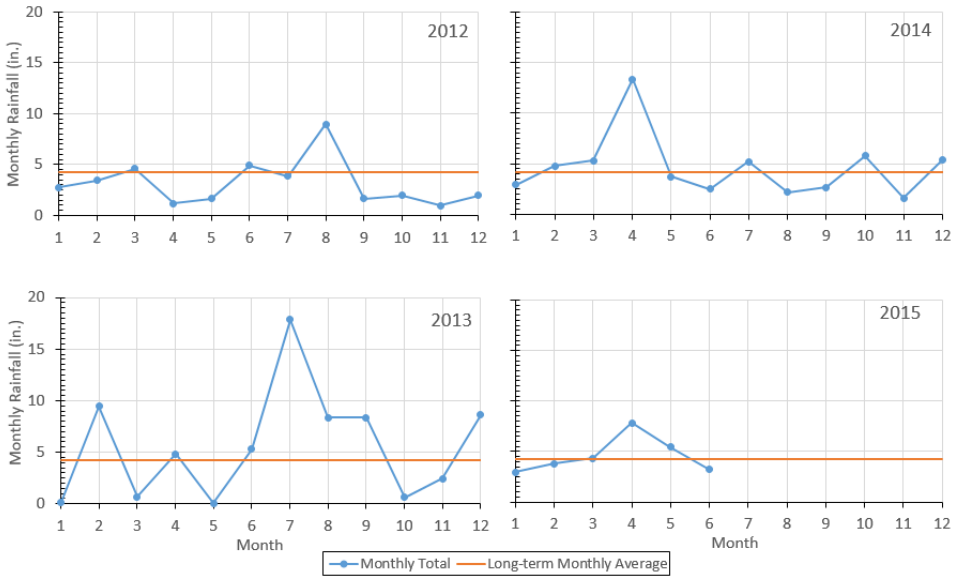


Figure 1.4: Monthly rainfall recorded at Dothan Regional Airport meteorological station since 2012. This meteorological station is 6.5 miles away from Dean Road Bridge

Moreover, as Figure 1.5 indicates, since 2011 there have been land use changes, including construction of structures and forest clear-cutting. These changes can help to increase processes such as surface erosion and streambank failures. This research will focus on numerical modeling approaches that attempt to describe the hydraulics of Soapstone Branch. This includes stream depth prediction, calculated shear stress and sediment transport through two-dimensional free surface flow modeling. This approach can achieve the final goal of the research via obtaining field data regarding the local hydrology and stream hydraulics, which were used to calibrate numerical models properly.

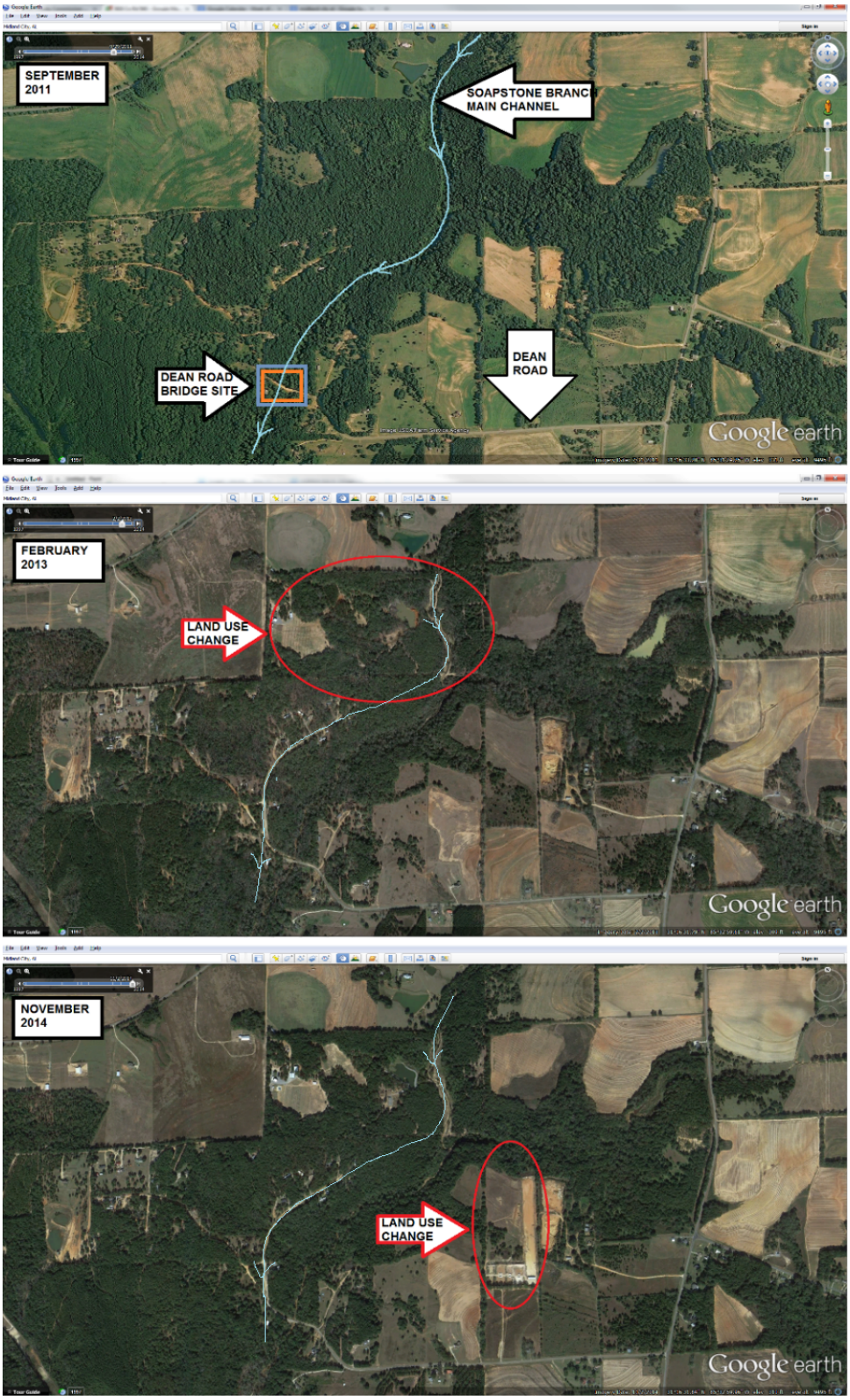


Figure 1.5: Land use changes identified in aerial images from Soapstone Branch watershed with reference to 09/2011 (top), in 02/2013 (middle), and 11/2014 (bottom).

# Chapter 2

## Research objectives

The aggradation of Dean Road Bridge caused by sediment carried by Soapstone Branch is severe, and it has resulted in overtopping following moderate-intensity rain events. This research will study this problem by focusing on proposing an alternative solution to the sediment blockage based on stream modification near Dean Road Bridge in order to improve the bridge conveyance characteristics.

The author was involved in this both field investigation and data analysis, including sensor deploying and data retrieving, and hydraulic model building, calibration, validation, DEM editing, and channel modifying. Sensors were deployed in the field and the data recorded by the sensor was retrieved by the author. Some sensors were relocated several time because of the bed elevation change in the Soapstone Branch. The author also built and calibrated the hydraulic models (HEC-RAS and SRH-2D) via the retrieved data from the field and government. Later, the models were then validated with a good result. In order to solve the aggradation problem nearby the bridge, flow velocity must increase, thus the bed slope must increase. In order to achieve these goals, DEM editing was conducted by the author to increase the longitudinal slope of the stream and to modify the cross-sectional geometry. Synthetic water flows were then used as the upstream boundary condition in the modified channel, and the results of those models were shown in this document.

It is anticipated that this investigation will provide insights in this type of problems, which is ongoing in other bridge structures in Alabama. With such knowledge, it is expected that solution strategies can be better devised for such structures. It is hoped that this work can help understand these conditions and with this propose recommendations to reduce the likelihood of aggradation in other bridge crossings.

# Chapter 3

# Literature Review

## 3.1 Aggradation in streams

Aggradation is a term used to describe the process of rising in river bed elevation. Most commonly, this is due to sediment deposition in a river system either by streambank instability, upland erosion processes, and other sources of sediment generation and transport. As it has been observed, the aggradation process created in Soapstone Branch at Dean Road Bridge crossing is so severe that the structure can be overtopped even when the watershed receives moderate rain events. Such overtopping events have the potential to cause structural damage, and even structural failure, with clear economical and human impacts.

Unlike scouring processes, which have received significant amount of research in past decades, there are not as many research contributions of aggradation in in-stream structures. The alternatives to control and eliminate aggradation in hydraulic structures as bridges are diverse, but not all are as effective, as pointed by Johnson et al. (2001). According to these authors, dredging is probably the simplest alternative, yet it is a continuous process that does not address causes of the problem and involves constant expenditures. Sediment trap construction upstream of bridges is another straightforward alternative, which can also accommodate the change of rate in sediment load in the future. Yet it requires continuous maintenance over its lifetime, and brings potential change to the local sediment budget in the stream. This in turn can lead to stream bed degradation in locations downstream from the trap and streambank instability.

Other more complex alternatives involve channelizing(Johnson et al., 2001) or adjusting stream slope near bridges and culverts. These one-time intervention must be considered with care to avoid issues related to scour. Also, this alternative may simply transfer aggradation issues downstream. Bridge replacement is also an even costlier alternative, and also requires

an estimate of what is the new stable sediment level in the stream, which in turn may not be straightforward or accurate.

### 3.2 Numerical tools to simulate river flows

A number of numerical modeling approaches have been developed to simulate rivers in the past five decades, and over time the range of the natural processes incorporated in the modeling tools have increased. At the current stage, river models are able to simulate backwater effects and unsteady flow processes, such as flooding events, considering one-dimensional (1D) or two-dimensional (2D) flow conditions. The influence of in-stream structures has also been incorporated in such models, as well as the ability of representing sediment transport. Also, over time, solution techniques for river flows have evolved from simple kinematic wave solution technique, into full solution of St. Venant equations (Cunge et al., 1980), and into non-linear numerical schemes (Glaister, 1988).

Various numerical models have been developed to represent a variety of open-channel flows, including flows in streams. Two of these models are focused in the present work, the US Army Corps of Engineers HEC-RAS 5.0 (River Analysis System) and the US Bureau of Reclamation SRH-2D (Sediment and River Hydraulics-2D). These models have capacity of representing two-dimensional flows and complex geometries((Brunner, 2010) and (Lai, 2008)). Considering the shallow characteristics of Soapstone Branch, such a feature is considered fundamental to this research.

The Hydrologic Engineering Center River Analysis System (HEC-RAS) is a 1D and 2D hydraulic model (Brunner, 2010) developed by the US Army Corps of Engineers that is able to simulate steady and unsteady river flows. The model capabilities also include sediment transport, movable boundary computations, in-stream structures and water quality parameters (Brunner, 2016). It has the ability of simulate long-term trends of scour and deposition in the stream in 1-D simulations. This system can be used to evaluate deposition in reservoirs, design channel contractions required to maintain navigation depth, predict the influence of dredging on the rate of deposition, estimate maximum possible scour during large flood events, and evaluate sedimentation in fixed channels (Brunner and Gibson, 2005).

The Sedimentation and River Hydraulics (SRH-2D) model is, according to Hogan (2015), a robust, finite-volume 2D model developed within the US Bureau of Reclamation (USBR). The model is able to simulate complex 2D river flow conditions (Lai, 2008), including sediment transport. The FHWA has partnered with the USBR to further develop SRH-2D and adopt this tool as a replacement to the outdated Finite Element Surface Water Modeling System (FESWMS) model (Hogan, 2015). While SRH-2D is able to perform sediment transport calculations, the goal is that this model is able to reproduce stream-structure interactions such as contraction scour in bridges.

At the foundation of these numerical models there is the mathematical model, which in turn is comprised by partial differential equations expressing mass and momentum equations, as well sediment motion processes. These two topics are focused in the following sections.

### 3.3 Mathematical formulation of hydraulic models

The St. Venant equations are a set of partial differential equations that describe conservation of mass and linear momentum in open-channel flow(Cunge et al., 1980).

$$\frac{\partial A}{\partial t} + \frac{\partial Q}{\partial x} = 0 \tag{3.1}$$

$$\frac{1}{A}\frac{\partial Q}{\partial t} + \frac{1}{A}\frac{\partial}{\partial x}(\frac{Q^2}{A}) + g\frac{\partial h}{\partial x} - g(S_0 - S_f) = 0 \tag{3.2}$$

where A is the cross sectional area of the open channel flow; Q is the flow rate; g is gravity; $S_0$ is bed slope and $S_f$ is frictional slope.

The Diffusion Wave equations are derived from the St. Venant equations through neglecting the local inertial and convective acceleration terms in the momentum. Thus the continuity equation (Equation 3.1) is unchanged. The momentum equation was simplified to the following form:

$$g\frac{\partial h}{\partial x} - g(S_0 - S_f) = 0 \tag{3.3}$$

In a two-dimensional (2D) hydraulic model, Shallow Water Equations need to be solved. Shallow Water equations are 2D version of St. Venant equations. The following equation is the 2D

version of continuity equation 3.1

$$\frac{\partial H}{\partial t} + \frac{\partial (hu)}{\partial x} + \frac{\partial (hv)}{\partial y} + q = 0 \tag{3.4}$$

where H is water elevation and h is water depth. H=h+z,where z is the bed elevation. Equation 3.4 is mass conservation equation. It can be the vector form:

$$\frac{\partial H}{\partial t} + \nabla * hV + q = 0 \tag{3.5}$$

where $V = (u, v)$ is the velocity vector and the differential operator $\nabla$ is the vector of partial derivative operators given by $\nabla = (\partial/\partial x, \partial/\partial y)$. q is the source term of the mass conservation equation. It could be rainfall, infiltration, or evaporation.

Following Brunner (2010) , integration over a horizontal region with boundary vector n can obtain the following equation

$$\frac{\partial}{\partial t} \iiint_{\Omega} d\Omega + \iint_{S} V \cdot n dS + Q = 0 \tag{3.6}$$

where $\Omega$ is the three-dimensional space occupied by the fluid. The side boundaries are given by S. Assuming that $\Omega$ is a function of H, the first term of equation 3.6 can be discretized as :

$$\frac{\partial}{\partial t} \iiint_{\Omega} d\Omega = \frac{\Omega(H^{n+1}) - \Omega(H^{n})}{\Delta t} \tag{3.7}$$

where the superscripts are the indexes of time. If the cells are assumed to have a polygonal shape, the boundary double integral of equation 3.6 can be written as a sum over the vertical faces of the volumetric region

$$\iint_{S} V \cdot n dS = \sum_{k} V_k \cdot n_k A_k(H) \tag{3.8}$$

where $V_k$ and $n_k$ are the average velocity and unit normal vector at face k and $A_k(H)$ is the area of face k as a function of water elevation.

Equations 3.7 and 3.8 can be substituted to equation 3.6 to obtain the following equation:

$$\frac{\Omega(H^{n+1} - \Omega(H^n)}{\Delta t} + \sum_k V_k \cdot n_k A_k(H) + Q = 0 \tag{3.9}$$

Bathymetry knowledge must be obtained before using this equation because $\Omega(H)$ and $A_k$ are functions of water elevation H. If the bathymetry information is not available, "box scheme" will recover it by assuming $\Omega(H) = P * h$ and $A_k(H) = l_k * h$ where $P$ is the area of the cell and $l_k$ is the length of the edge.

The Momentum Conservation equations for the Shallow Water Equations are derived from Navier-Stokes Equations through neglecting the baroclinic pressure gradients(variable density), strong wind forcing and non-hydrostatic pressure.

$$\frac{\partial u}{\partial t} + u\frac{\partial u}{\partial x} + v\frac{\partial u}{\partial y} = -g\frac{\partial H}{\partial x} + v_t(\frac{\partial^2 u}{\partial x^2} + \frac{\partial^2 u}{\partial y^2}) - c_f u + fv \tag{3.10}$$

$$\frac{\partial v}{\partial t} + u\frac{\partial v}{\partial x} + v\frac{\partial v}{\partial y} = -g\frac{\partial H}{\partial x} + v_t(\frac{\partial^2 v}{\partial x^2} + \frac{\partial^2 v}{\partial y^2}) - c_f v + fu \tag{3.11}$$

Equations 3.10 and 3.11 can be written in the following vector form:

$$\frac{\partial v}{\partial t} + V * \nabla V = -g\frac{\partial H}{\partial x} + v_t \nabla^2 V - c_f V + f \times V \tag{3.12}$$

In this equation, every term has a physical meaning. From left to right there is the unsteady acceleration, convective acceleration, barotropic pressure term, eddy diffusion, bottom friction and Coriolis term. The left hand side of the equation can be simplified using $\frac{DV}{Dt} = \frac{\partial V}{\partial t} + V * \nabla V$. The gravity term(g) was calculated using Somigliana formula:$g = g_0(\frac{1+ksin^2\varphi}{\sqrt{1-e^2 sin^2\varphi}})$ where $\varphi$ is latitude, $g_0$=9.780326 $(m/s^2)$,k=0.0019318514 is the normal gravity constant and e=0.0066943800 is the square of the eccentricity of the Earth. $v_t$ is the Eddy viscosity coefficient and it can be parameterized as $v_t = Dhu_*$ where D is a non-dimensional empirical constant with the value varying from 0.11 to 5 depending on the mixing intensity and geometry and surface of the channel. $u_*$ is the shear velocity, which can be computed as $u_* = \sqrt{gRS} = \frac{n\sqrt{g}}{R^{1/6}} \mid V \mid c_f$ is the bottom friction factor and it is given by $c_f = \frac{n^2 g|V|}{R^{4/3}}$ where

n is Manning roughness number. $f$ is the Coriolis parameter given by $f = 2\omega sin\varphi$ where $\omega$=0.0000729 is the sidereal angular velocity of the earth and $\varphi$ is the latitude.

In shallow frictional and gravity controlled flow; unsteady, advection, turbulence and Coriolis terms of the momentum equation can be disregarded to achieve a simplified version. Flow movement is driven by gravity and balanced by friction.

$$\frac{n^2 \mid V \mid V}{(R(H))^{4/3}} = -\nabla H \tag{3.13}$$

Dividing both sides of the equation by the square root of their norm, the equation can be rearranged into the following form:

$$V = \frac{-(R(H))^{2/3}}{n} * \frac{\nabla H}{|\nabla H|^{1/2}} \tag{3.14}$$

where V is the velocity vector, the magnitude of V is $\sqrt{u^2 + v^2}$, R is the hydraulic radius, $\nabla H$ is the surface elevation gradient and $n$ is the empirically derived Manning roughness number.

Equation 3.14 is derived from momentum conservation, yet it can be plugged into the mass conservation equation (equation 3.5) to get the Diffusion Wave Approximation of the Shallow Water equations(DSW)

$$\frac{\partial H}{\partial t} - \nabla \cdot \beta \nabla H + q = 0 \tag{3.15}$$

where $\beta = \frac{(R(H))^{5/3}}{n*|\nabla H|^{1/2}}$

If the bathymetry information is obtained, equation 3.14 can also be substituted into equation 3.9 to get the following equation:

$$\frac{\Omega(H^{n+1} - \Omega(H^n)}{\Delta t} + \sum_k \alpha \nabla H \cdot n + Q = 0 \tag{3.16}$$

where$\alpha = \alpha(H) = \frac{(R(H))^{2/3} A_k(H)}{n|\nabla H|^{1/2}}$. Once equation 3.16 was solved, the velocities can be solved by substituting H to equation 3.15.

SRH-2D was developed by the US Bureau of Reclamation (Lai, 2008). It has the feature of mobile bed sediment transport simulation in 2D, which was needed in this project. Unlike HEC-RAS, SRH-2D do not give the option to solve the diffusion wave equation. It solves 2D St. Venant equations only.

SRH-2D adopted the mass and momentum conservation equations in the following form:

$$\frac{\partial h}{\partial t} + \nabla \cdot (h\vec{V}) = 0 \tag{3.17}$$

$$\frac{\partial (h\vec{V})}{\partial t} + \nabla \cdot (h\vec{V}\vec{V}) = -gh\nabla z + \nabla \cdot (h\vec{\vec{T}}) - \frac{\vec{\tau}_b}{\rho} s \tag{3.18}$$

where $\vec{V}$ is the mean velocity vector, $\vec{\vec{T}}$ is the second order tensor of turbulence stress, $\vec{\tau}_b$is the bed shear stress vector, and $\rho$ is the fluid density.

Equations 3.17 and 3.18 can be integrated over a polygon using the Gauss theorem to yield:

$$\frac{\partial h\phi}{\partial t} + \nabla \cdot (h\vec{V}\phi) = \nabla \cdot (\Gamma \nabla \phi) + S_\phi^* \tag{3.19}$$

where $\phi$ stands for any dependent variable, $\Gamma$ stands for diffusivity factor, and $S_\phi^*$ is the source term. Equation 3.19 can be integrated over arbitrarily shaped polygon and the following equation is obtained:

$$\frac{(h_p^{n+1}\phi_p^{n+1} - h_p^n \phi_p^n)A}{\Delta t} + \sum (h_c V_c \mid \vec{S} \mid)^{n+1} \phi^{n+1} = \sum (\Gamma_c^{n+1} \nabla \phi^{n+1} \cdot \vec{n} \mid \vec{s} \mid) + S_\phi \tag{3.20}$$

where $V_c = \vec{V_c} \cdot \vec{n}$ and $S_\phi = S_\phi^* \cdot A$, $\vec{n}$ is the normal vector normal to $P_1 - P_2$ and $\vec{s}$ is the distance vector $P_1 - P_2$.

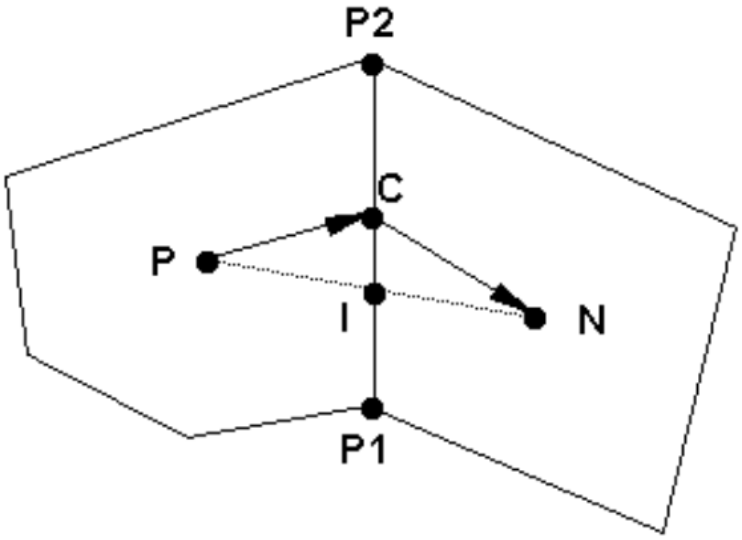


Figure 3.1: Schematic illustrating a polygon P along with one of its neighboring polygons N

The diffusion term in equation 3.20 is represented in the following way:

$$\nabla\phi\vec{n} \mid \vec{s} \mid = D_n(\phi_n - \phi_p) + D_c(\phi P_2 - \phi P_1) \tag{3.21}$$

where $D_n = \frac{|\vec{s}|}{(\vec{r}_1+\vec{r}_2)\cdot\vec{n}}$ and $D_c = -\frac{(\vec{r}_1+\vec{r}_2)\cdot\frac{\vec{s}}{|\vec{s}|}}{(\vec{r}_1+\vec{r}_2)\cdot\vec{n}}$. $r_1$ and $r_2$ are just vectors from P to C and from C to N.

Now if any variables needs to be calculated, for example, variable y, at center C, it should be calculated using the following interpolation. This interpolation is a second order accurate expression.

$$Y_I = \frac{\delta_1 Y_N + \delta_2 Y_p}{\delta_1 + \delta_2} \tag{3.22}$$

where $\delta_1 = \vec{r}_1 \cdot \vec{n}$ and $\delta_2 = \vec{r}_2 \cdot \vec{n}$ equation 3.22 calculates the Y value at point I, which can be used as the value at point C, because they are near to each other. But that is just a first-order accurate expression. The following equation is what makes it the second-order accurate equation.

$$Y_c = Y_1 - C_{side}(Y_{P_2} - Y_{P_1}) \tag{3.23}$$

where

$$C_{side} = \frac{\delta\vec{r}_2 - \delta\vec{r}_1)\vec{s}}{(\delta_1 + \delta_2) \mid \vec{s} \mid^2} \tag{3.24}$$

The $\phi_c$ term in equation 3.20 needs further discussion. Large oscillations may occur with second order scheme employed directly. Thus a damping term should be added. The damped scheme is derived by blending the first order upwind scheme with second order central difference scheme/

$$\phi_c = \phi_c^{CN} + d(\phi_c^{UP} - \phi_c^{CN} \tag{3.25}$$

where $\phi_c^{UP} = \frac{1}{2}(\phi_p + \phi_N) + \frac{1}{2}sign(V_c)(\phi_p - \phi_N)$ and the $\phi_C^{CN}$ term comes from the interpolation process from equation 3.22 and 3.23. d is the damping value from 0.2 to 0.3.

The final governing equation for element P is as following:

$$A_P\phi_P = \sum_{nb} A_{nb}\phi_{nb} + S_{diff} + S_{conv} + S_\phi \tag{3.26}$$

Here the notation "nb" refers to "neighbor" and the following are the explanation of terms in equation 3.26

$$A_{nb} = \Gamma_C D_n + \max(0, -h_c V_c \mid \vec{s} \mid)$$

$$A_p = \frac{h_P^n A}{\Delta t} + \sum_{nb} A_{nb}$$

$$S_{diff} = \frac{h_P^n A}{\Delta t} + \sum$$

$$S_{conv} = \sum_{allsides} (h_c V_c \mid \vec{s} \mid)((1-d)(\frac{\Delta_1}{\Delta_1 + \Delta_2} - \frac{1 - sign(V_c)}{2})(\phi_N - \phi_P))$$

The following procedure may be needed to avoid checkerboard instability for a non-staggered mesh to obtain the polygon side normal velocity. The operator "<>" is defined here as interpolation using the method in 3.22. If a vector is interpolated, it means the interpolation is applied to each Cartesian component of the vector.

$$V_c = < \vec{V} > \cdot\vec{n} + < \frac{A}{A_P} >< gh\nabla z > \cdot\vec{n} - < \frac{A}{A_P} > gh\nabla z \cdot \vec{n} \tag{3.27}$$

If the elevation $Z^*$is known from previous time step or initial condition, an intermediate v can be calculated using the following equations.

$$A_P\vec{V}_P^* = \sum_{nb} A_{nb}\vec{V}_N - a\nabla Z^n + \vec{S}_V \tag{3.28}$$

where one also has:

$$\vec{V'} = V^{n+1} - \vec{V}^*$$

$$Z' = Z^{n+1} - Z^n$$

which will have the momentum equations satisfied, i.e.

$$A_P V_P^{n+1} = \sum_{nb} Anb\vec{V}_N^{n+1} - a\nabla Z^{n+1} + \vec{S}_V$$

Or

$$A_P V_P' = \sum_{nb} A_n b\vec{V_n'} - a\nabla Z'$$

With SIMPLEC algorithm (Patankar, 1980), the above equations may be approximated as:

$$\vec{V_P'} = \frac{a}{A_p - \sum_{nb} A_{nb}}\nabla Z' \tag{3.29}$$

Equation 3.29 can be plugged into equation 3.17 to get the following equation:

$$\frac{Z'}{\Delta t} + \nabla\cdot(\vec{V}Z') = \nabla(\frac{ah}{A_p - \sum_{nb} A_{nb}}\nabla Z') - \nabla\cdot(h^n\vec{V^*}) \tag{3.30}$$

Z can be solved through equation 3.30, and through plugging equation 3.30 to equation 3.29, V can also be solved.

In a typical iterative solution process, momentum equations are solved first assuming known water elevation and turbulent viscosity given at the previous time step. The newly obtained velocity is used to calculate the normal velocity at mesh element sides in equation 3.28. This side velocity will usually not satisfy the continuity equation. Therefore, the pressure correction equation 3.30 is solved and equation 3.29 is used to obtain a new elevation and new

velocity. After the elevation correction equation, other scalar equations, such as turbulence and sediment equations, may be solved. This completes one iteration of the solution cycle. According to Lai (2008) the engine is very robust and stable.

### 3.4 Modeling aggradation processes

An important component to enable a numerical model is an adequate mathematical model describing the process of aggradation. One of those such models was been developed by Zhang and Kahawita (1987). The authors derived two fundamental equations such as linear momentum conservation and continuity equations for water, continuity equation for sediment, sediment transport relation, and resistance relation. And the equations that they derived are as following:

$$\frac{\partial Z}{\partial t} - K_1\left(\frac{\partial^2 Z}{\partial x^2} + 1/g\frac{\partial^2 E}{\partial x^2}\right) = 0 \tag{3.31}$$

$$\frac{\partial G}{\partial t} - K_1\frac{\partial^2 G}{\partial x^2} = 0 \tag{3.32}$$

$$K_1 = \frac{\partial G}{\partial s}\frac{1}{1-\lambda} = \frac{bG_0^{1-\alpha}G^{\alpha}}{3s_0(1-\lambda)} = K_0 G^{\alpha} \tag{3.33}$$

Where $Z$ is change in bed elevation; $K_1$ is linear diffusion coefficient; $g$ is acceleration of gravity; $E$ is specific energy ($u^2/2 + gh$); $G$ is charge per unit width; $\alpha$ is dimensionless factor; and $\lambda$ is bed material porosity.

Further analytical solution and experimental verification were performed by Zhang and Kahawita (1987). An analytical solution for prediction of one-dimensional non-equilibrium processes in alluvial rivers due to a sudden constant increase in upstream sidemen discharge was presented by the authors. One limitation of this study is that all the tests were performed in laboratory conditions. There have been additional work in developing solutions for aggradation and degradation processes in artificial channels. Unsteady flow and solid transport simulation processes in artificial channels can be solved using a three-equation model, coupled with a local erosion law. Aricò and Tucciarelli (2008) derived this method to couple the scour and erosion

effectiveness into three main equations (momentum equation, continuity equation, solid load balance equation).

By comparison with aggradation research, much more effort was dedicated to experimental and numerical modeling of river sediment transport processes. According to Yang (1996), the initial mathematical model formulations in this area dated from the 1950s, combining aspects of fluid dynamics and empirical sediment-water relations. Numerical 1-D sediment transportation models had been used frequently in the context of rivers, and more recently 2D models are being introduced. Sediment transportation models are becoming more complex, including non-uniform and non-equilibrium models. Yet, the most commonly used model is still the 1-D model since it requires less measured data and yields more stable results. HEC-RAS can do both 1-D and 2-D modeling and it is also able to predict a long term sediment transportation, but can only simulate 1D sediment transport. An examples of large-scale, long-term sediment transport simulation using HEC-RAS was provided by Ghimire and DeVantier (2016).

This chapter described some of the past contributions in aggradation processes, as well as mathematical and numerical modeling of river flows. It provided a theoretical background to support the discussion that follows in the next chapter, which will focus on how these modeling tools were implemented in the context of Dean Road Bridge.

# Chapter 4

# Methodology

One alternative to understand and address problems related to aggradation in hydraulic structures is through the development and calibration of hydraulic models. Hydraulic models can represent and predict the real situation at the site. Through tuning the parameters of the models, researchers can easily see the results of the tuning and choose the best of them. This chapter is divided to two sections: data gathering and field investigation; and hydraulic modeling. The data gathering and field investigation section has the following subsections: bridge cross section survey; soapstone branch digital elevation model; precipitation and evapotranspiration data collection; particle size distribution characterization; stream flow depth and velocity data collection; and sediment sampling during rain events. The hydraulic modeling work section has the following subsections: initial and boundary conditions for hydraulic calculation; digital elevation model editing; mesh generation; and hydraulic model calibration.

## 4.1 Data gathering and field investigation

### 4.1.1 Bridge cross section survey

Upon the start of the research, ALDOT provided a history of surveys in the bridge cross section since 1992, which is presented in Figure 4.1. As is indicated the aggradation process had become noticeable in 2013, and by 2014 the entire cross section was blocked with sediments. Despite of efforts to dredge the bridge in February 2015, by August 2015 the entire cross section was blocked again, as was shown in Figure 4.1.

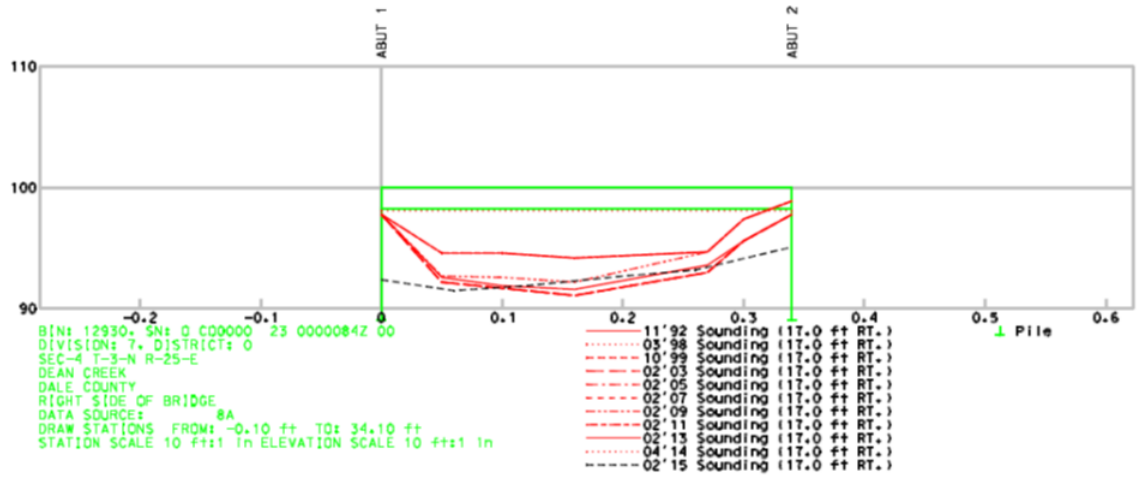


Figure 4.1: History of the Dale County Bridge (BIN 12930) cross section from 11/1992 to 02/2015. Aggradation is noticeable from 02/2013 onward, with a dredging occurring in 2015.

### 4.1.2 Soapstone branch digital elevation model

Dale County provided means to develop a digital elevation map (DEM) of Soapstone Branch, which is presented in Figure 4.2. The 10 m DEM obtained from USGS NED 30 is very coarse for the Soapstone Branch catchment. In the case of large to medium size catchments like the donor catchment (Choctawhatchee river catchment draining near Newton, Alabama covers an area of 686 square miles), a coarser resolution DEM can be utilized without producing errors of higher degrees. However, due to the small size of Soapstone branch, a finer resolution DEM is required. A contour shapefile with a 2 foot interval of Choctawhatchee river catchment was obtained from Dale County. This contour shapefile was then converted to 1 m resolution DEM using a software tool such as ArcGIS (ESRI, 2011)

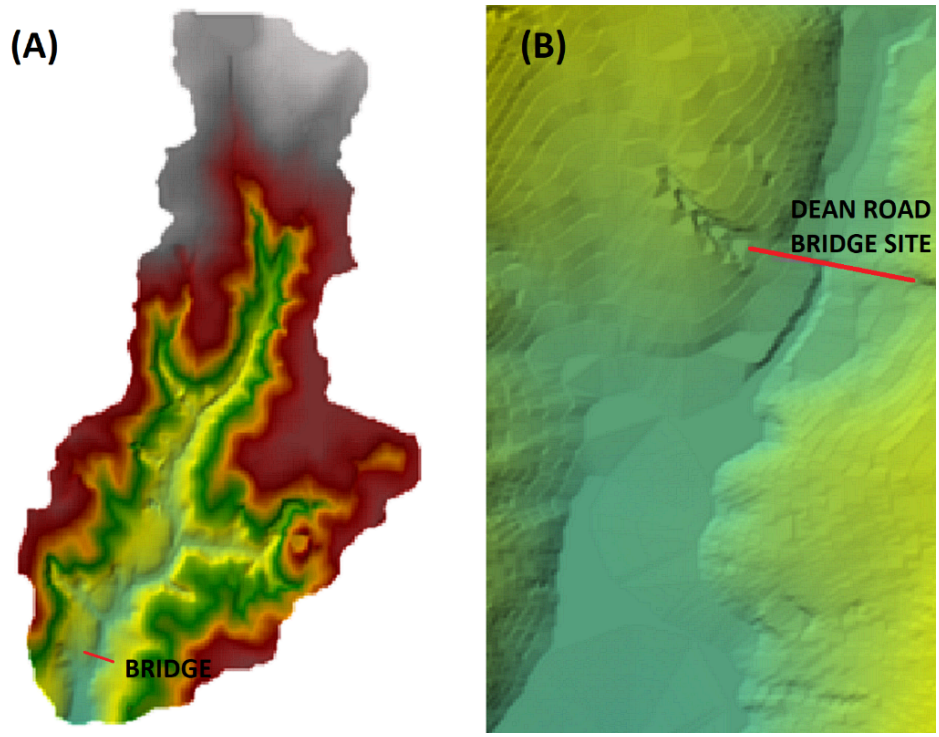


Figure 4.2: Digital elevation map (2 ft. resolution) of Soapstone Branch Watershed (A), magnified near the bridge site (B)

### 4.1.3 Precipitation and evapotranspiration data collection

Rainfall data collection is fundamental for the development of both hydrological and hydraulic data. Rainfall data from 01/2009 to 02/2016 used in this research was obtained through a rain gauge nearby at the Dothan Airport, AL. From 02/2016 onward, rain data was collected on site using ONSET RG3 tipping bucket rain gauges installed through this research. The location of the rain gauges is presented in Figure 4.1.3, along with the picture showing one of the rain gauges installed in the study area. Through a combination of the Dothan Rainfall data and the locally collected rainfall time series, presented in Figure 4.4, was developed and used in the research.

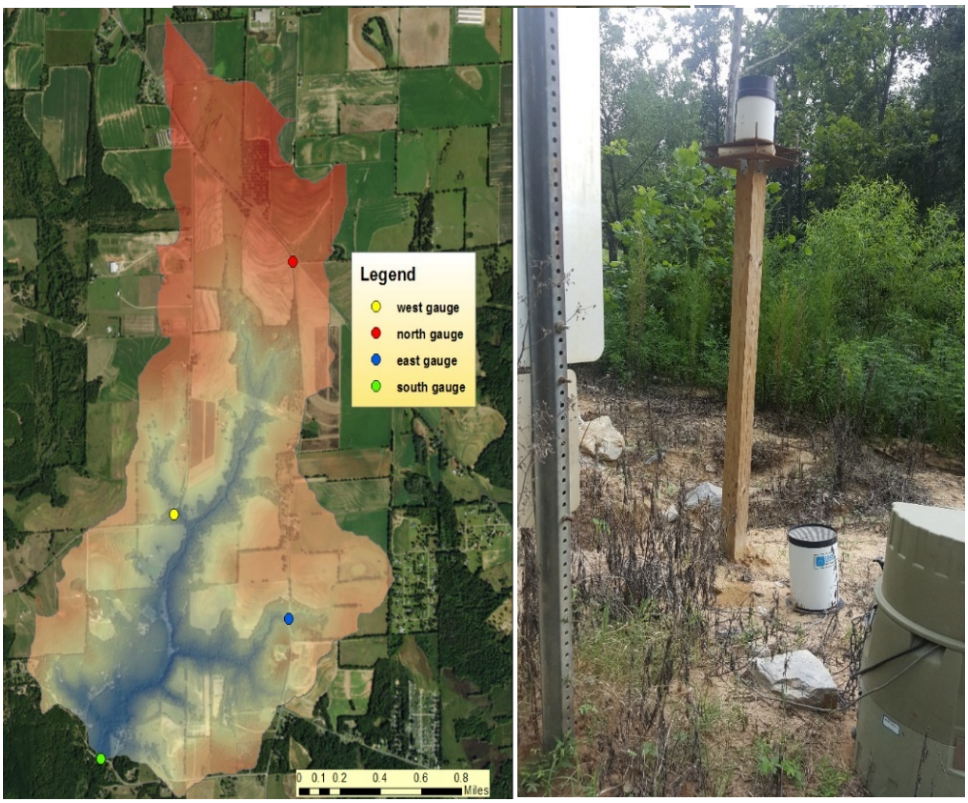


Figure 4.3: Rain Gauge Locations in the Catchment (Left) and installed rain gauge (Right). The ONSET RG3 rain gauge can be seen in the top of the post, whereas another ISCO rain gauge (used with the autosampler) is shown in the bottom (Tamang, 2017).

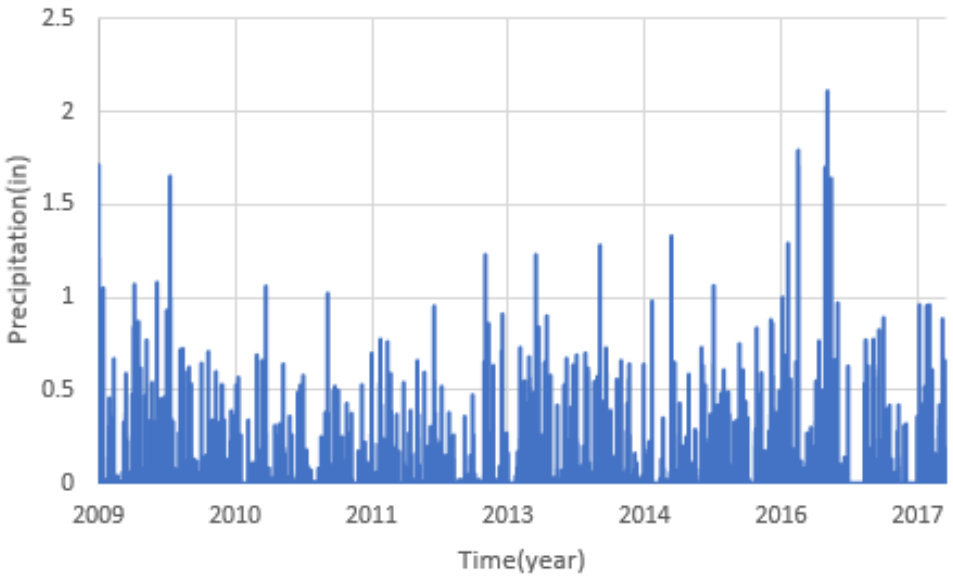


Figure 4.4: Precipitation Data used for HEC-HMS collected by Rain Gages

The ONSET rain gauge has a water collecting tipping bucket, and whenever the bucket is full, the bucket falls and tips the metallic connection at the bottom, and the rain gauge will consider this tipping as 0.01 inch of rain. The rain gauge can be connected to the computer through a data shuttle. This and other types of ONSET sensors are typically deployed for outdoor research. They have only one optical COM port on them to communicate with a computer. The data shuttle is hardware that can transfer optical signals to digital signals that can be read by computers. The right side of Figure 4.5 are the couplers that connect the sensor and the shuttle. The coupler creates a dark environment to enable optical communication.


Figure 4.5: ONSET rain gauge(A) and its couplers(B)

Daily pan evapotranspiration data were obtained for stations located in Headland, AL for the period of 2009-2013. For years 2014-2016 and days with missing values, monthly average pan evapotranspiration data from Class A pans for the closest station (i.e., Martin Dam) provided by the National Oceanic and Atmospheric Administration - NOAA (Farnsworth and Thompson, 1983) were used. A correction factor of 0.7 is applied to convert pan evapotranspiration to potential evapotranspiration.

### 4.1.4 Particle size distribution characterization

Soil samples were collected at various locations at Soapstone Branch and grain size distribution tests were performed in these samples, with results presented in Figure 4.6. The location where these samples were collected are presented in Figure 4.7, and are mostly concentrated near the bridge site.

All samples consisted mostly of sand-sized particles by mass, with one sample having 17% of gravel sized particles and another sample containing 28% of silt/clay size particles. These results suggest that most sediments in the watershed are non-cohesive (Briaud, 2004), which is a relevant finding for the hydraulic modeling studies.

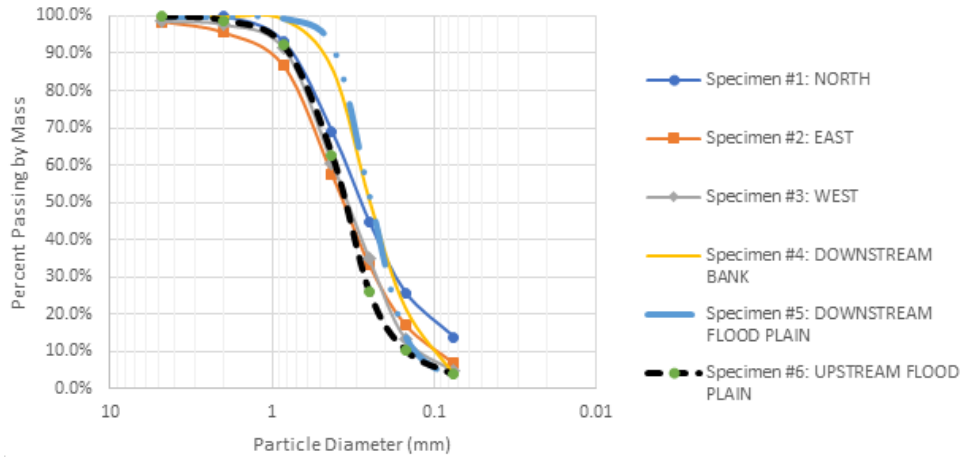


Figure 4.6: Particle size distribution of different soil samples obtained in the Soapstone Branch Watershed

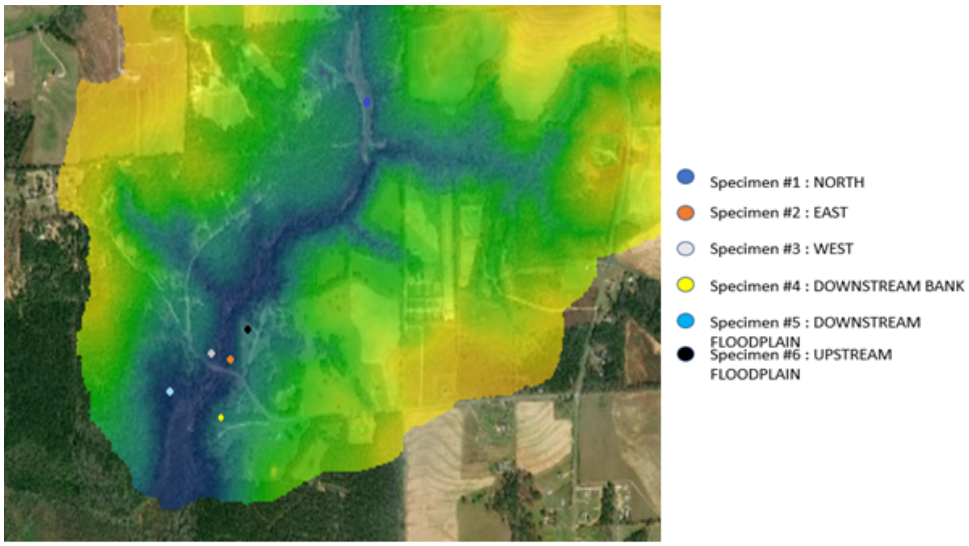


Figure 4.7: Locations where soil samples were taken within Soapstone Branch Watershed.

### 4.1.5 Stream flow depth and velocity data collection

Parameters such as the local topography, precipitation and evaporation data, land use and soil characteristics will influence runoff generation and then change stream flow depth and velocity during a given rain event. In order to characterize these variables within Soapstone Branch, different sensors were used. Level loggers ONSET HOBO U20L (Figure 4.8), sampling every 15 minutes, were used to characterize flow depth in stream cross section.


Figure 4.8: HOBO Water Level Logger 13ft U20L

A Teledyne 2150 AV (area-velocity) sensor (Figure 4.9) was used to collect water velocity and water depth data immediately upstream the bridge site. The HOBO U20L sensors measured pressure at the stream bed, and thus required atmospheric pressure correction, and an U20L sensor gauging atmospheric pressure was placed in together with the rain gauge near the bridge site. The 2150 AV sensor has built-in atmospheric correction, and does not need atmospheric data gathering.

Figure 4.9: Teledyne 2150 AV sensor used in this research, with data acquisition box, battery and connecting cable.

One problem that could not be solved in this research was the measurement of stream flow velocity with the AV sensor. The sensor uses Doppler effect to track motion of particles within the flow and with this determines the stream velocity. Because of large amounts of sediment carried with the stream flow, particularly during rain events, the AV sensor was often buried and thus could not record velocity (even though pressure recording was still possible). As shown

in Figure 4.10, for many long periods the AV sensor velocity was zero or even negative, which was not feasible.

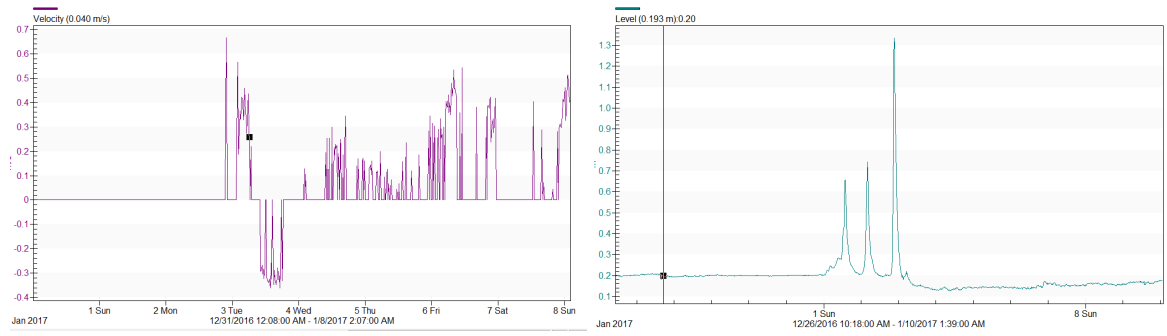


Figure 4.10: Results from velocity measurements with AV sensor. Zero and negative velocities are attributed to the Soapstone Branch sediment load burying the sensor.

Different methods of deployment were tried but none of them succeeded on locating a place where the AV sensor can be deployed without being buried for a relatively long time (several events). Figure 4.11 shows the AV sensor was deployed on the bridge pier. The sensor was sitting on the stream bed clamped to the bridge pier, and the water is overtopping the sensor for less than half inch. And that water depth is deeper than other places near the bridge. There was no place where the water depth was big enough that the change on the bed elevation due to sediment transportation could be neglected.

Figure 4.11: Teledyne 2150 AV sensor

### 4.1.6 Sediment sampling during rain events

This research intended to establish a relationship between turbidity levels measured in the stream and the concentration of sediments in the flow, characterized by the Total Suspended Sediments (TSS) parameter. To attain this goal, a Teledyne ISCO 6700 Autosampler, shown in Figure 4.1.6, was deployed in the bridge site to perform sample collections. Samples collected within the bottles of the autosampler were later taken back to Auburn so that TSS tests were made, along with turbidity measurement.


Figure 4.12: Teledyne ISCO 6700 Autosampler used in turbidity and TSS characterization of samples taken from Soapstone Branch during rain events.

An alternative way for sediment characterization was also attempted by using a turbidity sensor, model INW Turbo, with range up to 3000 NTUs, shown in Figure 4.1.6. This sensor was also placed in the bottom of Soapstone Branch next to the AV sensor that was measuring stream velocity. However, like the AV sensor, it was frequently buried by the Soapstone Branch sediments and did not provided useful data.

Figure 4.13: INW Turbo turbidity sensor, with logger box, that was used in the Soapstone Branch sediment characterization. Sediment loading covered the sensor head (black), preventing the correct sensor operation.

## 4.2 Hydraulic modeling

### 4.2.1 Initial and boundary conditions for hydraulic calculation

The initial condition adopted for all hydraulic models (HEC-RAS and SRH-2D) was to assume that stream was dry, which then required that models were run for enough time until base flow conditions were attained. One point to make is that the numerical scheme used by HEC-RAS is not unconditionally stable. If the guessed initial water elevation is too far away from the actual situation, it could cause the model to diverge.

The upstream boundary condition used by both models is the discharge time-series obtained by HEC-HMS. Such flows at a location near the bridge site was copied from HEC-HMS output and used as a time series in the hydraulic models. The downstream boundary condition for both models, located far downstream from the bridge location, assumed a normal flow condition with an energy slope of 0.5%. While HEC-RAS also has the ability of allowing inflows

from precipitation, albeit without abstractions, this was not used in the present effort. A typical HEC-HMS outflow data, which was used as an upstream boundary condition, is presented in Figure 4.14.

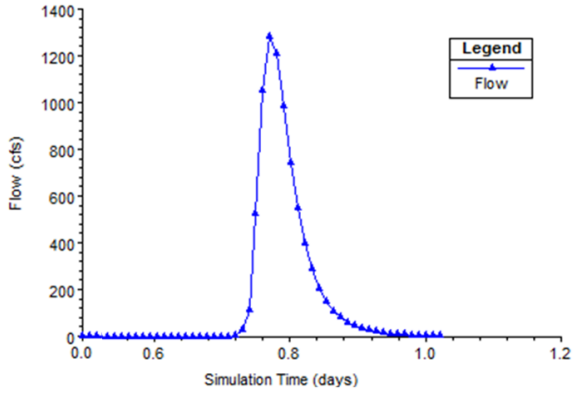


Figure 4.14: HEC-HMS outflow data on 09JUL2016, used as upstream boundary condition in the hydraulic models

### 4.2.2 Digital elevation model (DEM) editing

Two-dimensional hydraulic models rely heavily on topographical information to determine flow paths, depths, velocity, among other flow variables. DEM data may have some shortcomings that require adjustments before a hydraulic modeling can be used. One typical limitation is the presence of a bridge, since the stream cross section underneath the bridge deck is not represented. Also, in the case of a stream that has a very large amount of sediment load, one expects changes in its morphology. Due to these limitations, it was necessary to edit the DEM obtained from Dale County near the site of Dean Road Bridge.

The original DEM was clipped to a relatively small data file with only about 700m along the reach. The upstream boundary of the clip is about 100 meters away from a station where flow data was obtained from HEC-HMS. The stream bed profile along the reach was incorrectly depicted in the DEM, with a lot of cliffs and adverse slope. The various field trips to the site helped to indicate to the research team that the stream slope was mostly uniform. Thus, the channel slope must be corrected before the modeling. It was assumed 0.5% slope for Soapstone Branch based on these field site observations. Figure 4.15 presents the changes implemented in the DEM near the bridge site by showing the stream profile at the center of Soapstone Branch.

The same methodology for DEM editing was also used to perform changes in the model and enable the study of alternative cross sections to evaluate stream modification strategies.

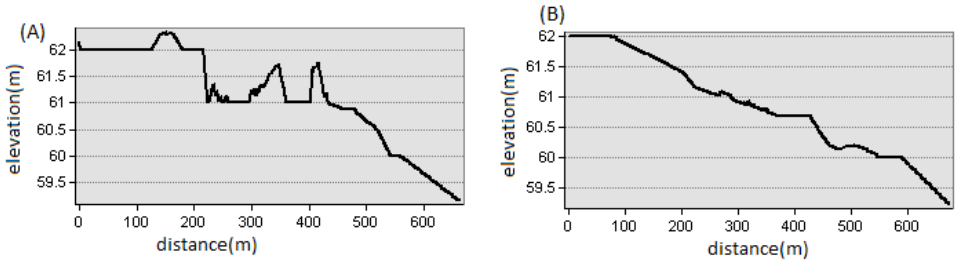


Figure 4.15: Profile of the centerline of Soapstone Branch before (A) and after (B) the DEM editing process to eliminate inconsistencies observed in the original DEM data file. Dean Road Bridge is at the location 300 m, and originally was blocking the river flow

### 4.2.3 Mesh generation

The HEC-RAS model has a uniform structured mesh with the size of 3m by 3m. Yet the mesh near the channel was unstructured and inconsistent. To make sure there would be enough mesh in the channel, at least 5 longitudinal breaklines were added along the channel so that there will be at least 5 computational cells in the channel at any station. A breakline is a line drew by the modeler representing a road or a bridge to ensure that computational cells are aligned with these features. However, a secondary effect of enforcing a breakline in HEC-RAS is that the mesh is locally refined. This was used in the present modeling effort, so that there were more computational points within the Soapstone Branch channel, as is shown in Figure 4.16.

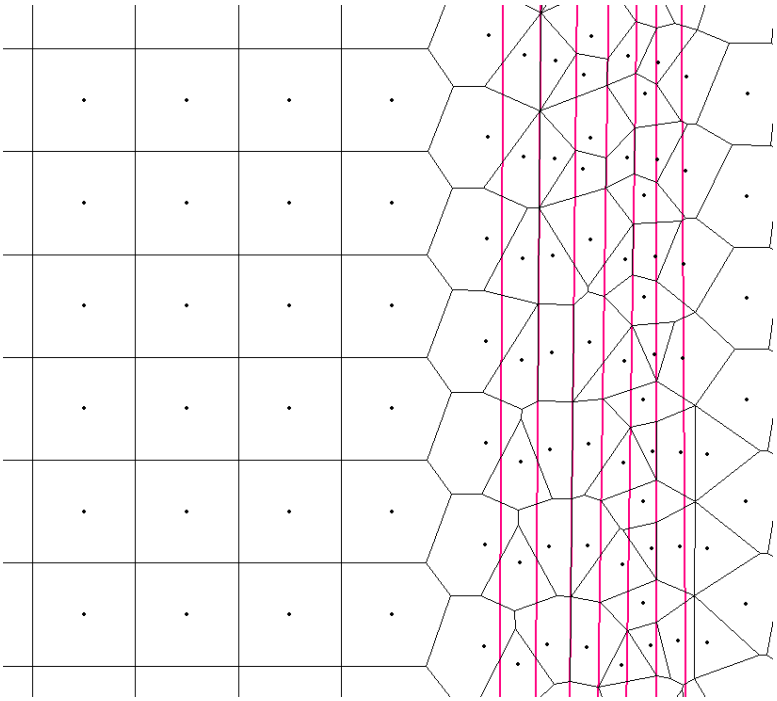

Figure 4.16: Section of the HEC-RAS mesh used for the modeling of Soapstone Branch, indicating breaklines and a finer mesh to the right, where the stream channel is located.

Regarding mesh generation for the SRH-2D model, it relies on a pre-processing tool called Surface-water Modeling System, or SMS (Aquaveo, 2017). SMS generates triangular and quadrangular mesh for a SRH-2D model, and in the case of the present work a triangular, unstructured mesh was used, in which the maximum distance between the grid points in the mesh was adopted as 5 m, with a smaller maximum distance of 1.5 m used at the Soapstone Branch channel. Figure 4.17 depicts a section of the mesh used by SRH-2D to represent Soapstone Branch.

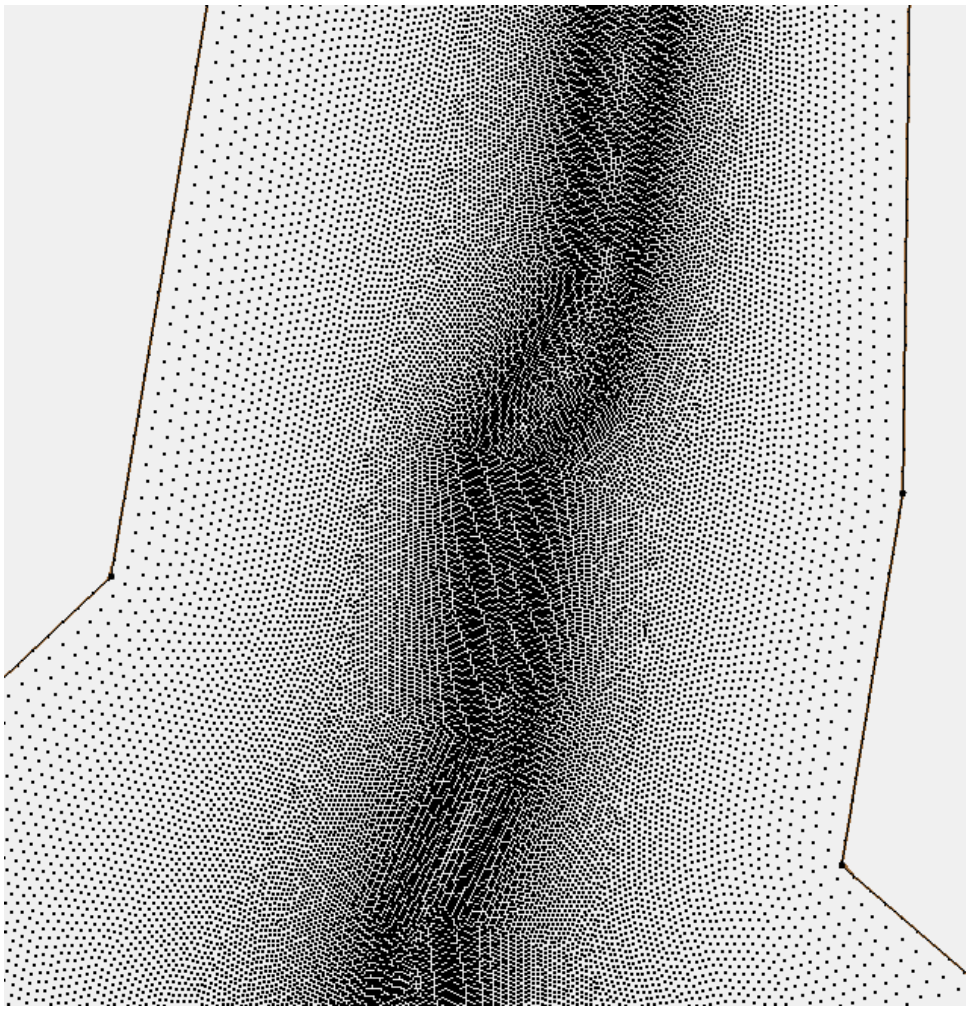

Figure 4.17: Section of the SRH-2D grid points from the mesh generated through SMS, showing how the points are more spaced as it distances from the channel.

### 4.2.4 Hydraulic modeling calibration

With adequate upstream inflow information, topographical and a developed mesh it is possible to initiate the process of hydraulic modeling calibration. In the case of 2-D models this is comparatively simpler than the calibration of 1-D models, since there are fewer assumptions needed for model development. For instance, in the case of flows approaching a bridge in 1-D HEC-RAS model, it is necessary to make assumptions of ineffective flow areas. Such is not needed in the case of 2-D modeling with HEC-RAS.

Typically, the main calibration parameter for a stream model is linked to the bed roughness, as this impacts depth profiles. In the case of Soapstone Branch there is an advantage in that the

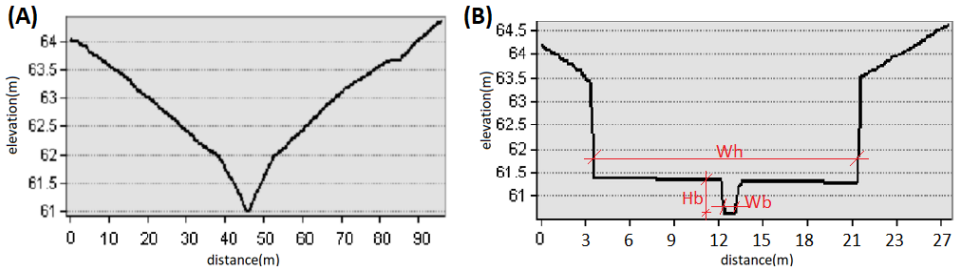


Figure 4.18: Original and edited stream cross section near the bridge site. The edited geometry cross section parameters are presented in the right. The other selected calibration parameter was the Manning roughness n.

types of land covers in the hydraulic modeling area is mostly comprised of forested areas and stream banks. However, there was a practical difficulty posed by the actual Dean Road Bridge and the aggradation that happens in it. During moderate to large rain events, the stream receives enough inflow to increase its velocity. Large velocities in the stream enable a partial sediment removal under the bridge deck, which increase its conveyance. As inflows keep increasing, the bridge is overtopped, and flows go either on the top or in the bottom of the bridge. This is a very complex situation, and cannot be modeled without resorting to a calibration process.

The strategy to represent the hydraulic behavior of the existing bridge cross section conveyance was to create a unique representation for the bridge cross section that was based on a two-tier discharge structure. The lower tier would be able to adequately reproduce the conditions of flow depth associated with low flows and base flows, and the upper tier with more intense stream flows. This was implemented also by editing the DEM near the bridge site, and Figure 4.18 presents the resulting elevation data after this editing was completed.

The process of selecting the geometric characteristics of the double-trapezoid cross section of Figure 4.18 was the key part of the hydraulic modeling calibration. The calibration variables included: low-flow bottom width (Wb), assumed as either 4 ft. or 5 ft.; the low-flow channel height (Hb), assumed as 0.5 ft., 0.7 ft. or 0.9 ft. The width of the high flow channel (Wh) was assumed either 20 ft., 40 ft. or 60 ft. The side slopes for both channels were set at $m$ = 2 (2 horizontal: 1 vertical). Finally, Manning number was assumed as either $n$ = 0.020, $n$ = 0.025 and $n$ = 0.030. In total, more than 50 different combinations of these variables were considered,

and these geometries were tested in a selected group of rain events presented in Table 4.1. The best agreement between observed and simulated depth hydrographs was attained when Wb = 4 ft., Hb = 0.7 ft., Wh = 60 ft. and $n$ = 0.025. An example of a flood event is presented in Figure 4.19 showing modeled and simulated depth hydrographs (using HEC-RAS) for three different set of calibration values..

Table 4.1: Rain events recorded in Soapstone Branch Watershed and used for hydraulic modeling calibration

| Rain event | Date |
|---|---|
| 1 | 16-Jun-16 |
| 2 | 9-Jul-16 |
| 3 | 3-Aug-16 |
| 4 | 13-Dec-16 |
| 5 | 1-Jan-17 |
| 6 | 7-Jan-17 |
| 7 | 21-Jan-17 |

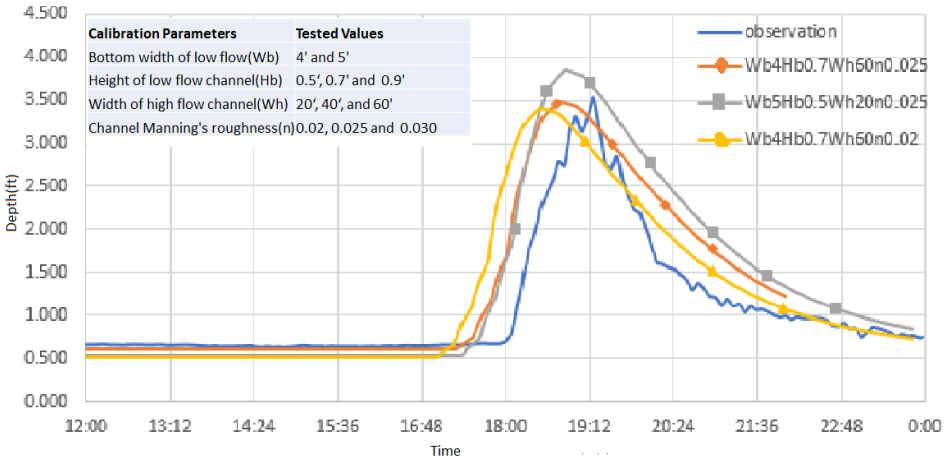


Figure 4.19: Typical Calibration Results

# Chapter 5

# Results and Discussion

Starting from the hydrological modeling results, the hydraulic modeling of free surface flow intends to assess the ability of modified stream geometries near Dean Road Bridge to transport sediments and avoid aggradation. This is achieved in three steps. Initially, the hydraulic models were assessed in their ability of reproducing stream depth changes based on the HEC-HMS output, which in turn was obtained with rainfall data collected on site. The HEC-HMS outflow hydrographs were used as input data for HEC-RAS 5 or SRH-2D, according to analysis objective. The second step was to focus on studying modeled flow velocity and shear stress results obtained near Dean Road Bridge in its current condition and after a stream modification. Finally, the ability of the proposed stream modification of avoiding sediment retention is tested with the use of hydraulic modeling accounting for sediment transport.

## 5.1 Assessment of model ability to represent hydrographs

HEC-RAS results of depth hydrographs upstream from Dean Road Bridge for two calibration rainfall events are presented in Figures 5.1 and 5.2. Figures 5.3 and 5.4 present the comparable results for the model validation dataset. It is possible to assess that these events have varying intensities, since the stream depth changes ranges from 1.5 ft. up to 4 ft. As pointed earlier, the geometric characteristics of the bridge cross section (Figure 4.18b) were varied to improve the accuracy of peak stream depth representation. Figures 5.3 and 5.4 present the final calibration results using the following channel geometry: Wb = 4 ft., Hb = 0.7 ft., Wh = 60 ft. and n = 0.025 (Figure 4.18b). All validation dataset errors were assessed with this set of parameters.

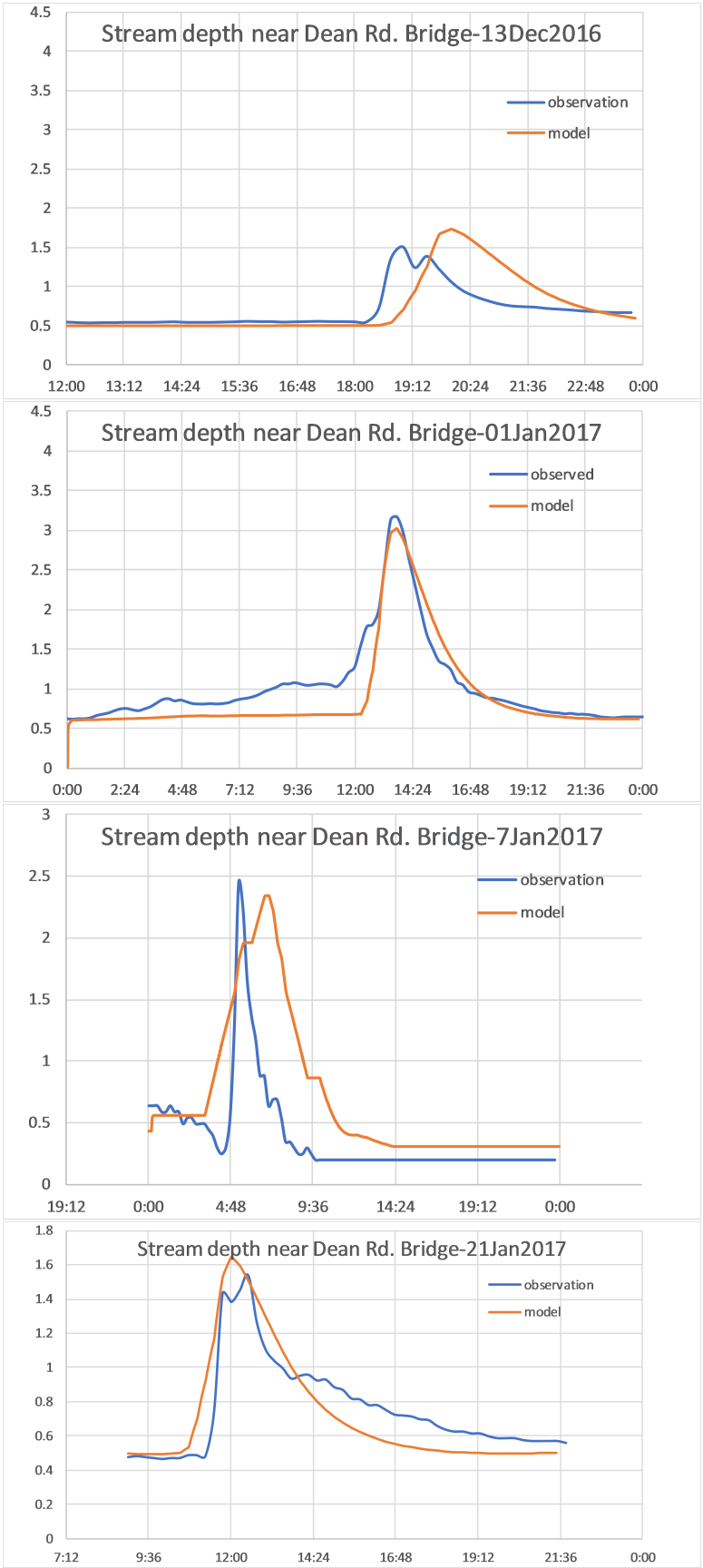


Figure 5.1: Stream depth hydrographs observed in Soapstone Branch and modeled with HEC-RAS 5 for four validation rainfall events in late 2016 and early 2017 using outflows modeled by HEC-HMS.

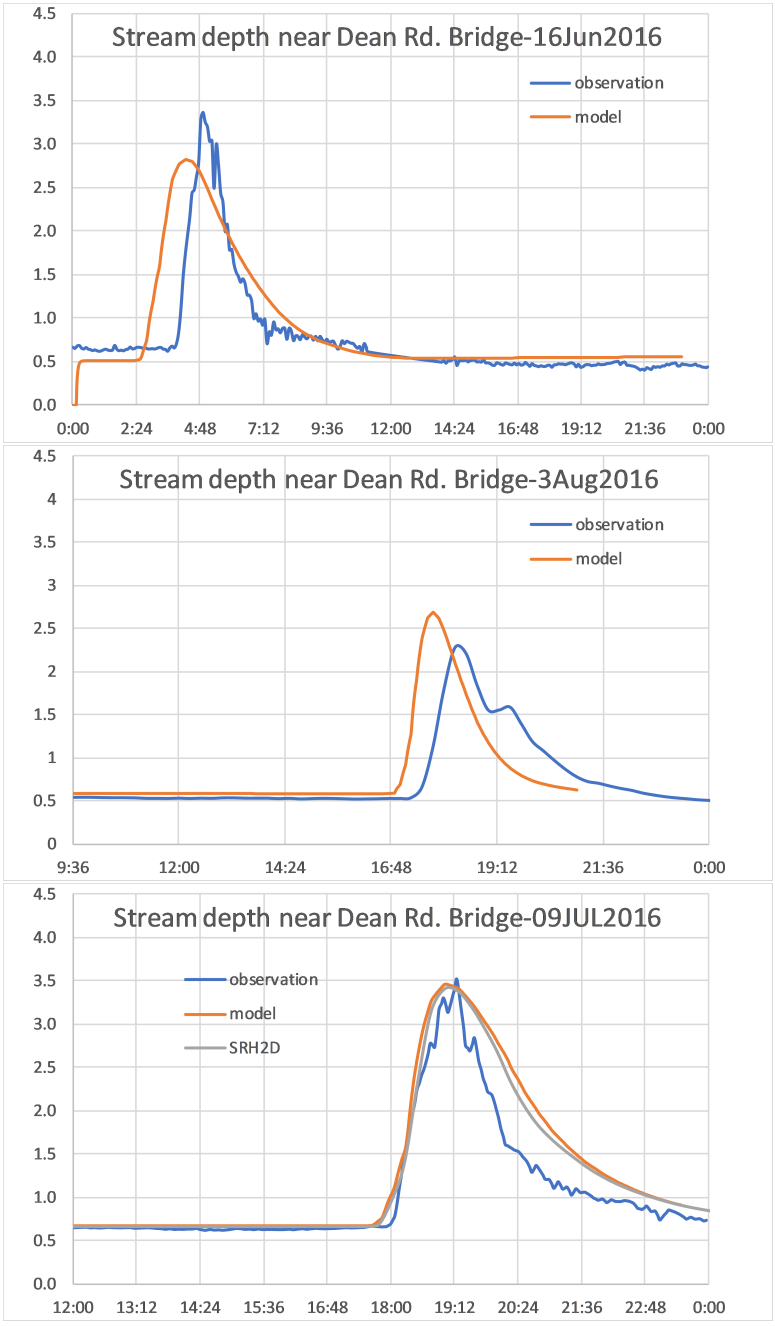


Figure 5.2: Stream depth hydrographs observed in Soapstone Branch and modeled with HEC-RAS 5 for three validation rainfall events in 2017 using outflows modeled by HEC-HMS

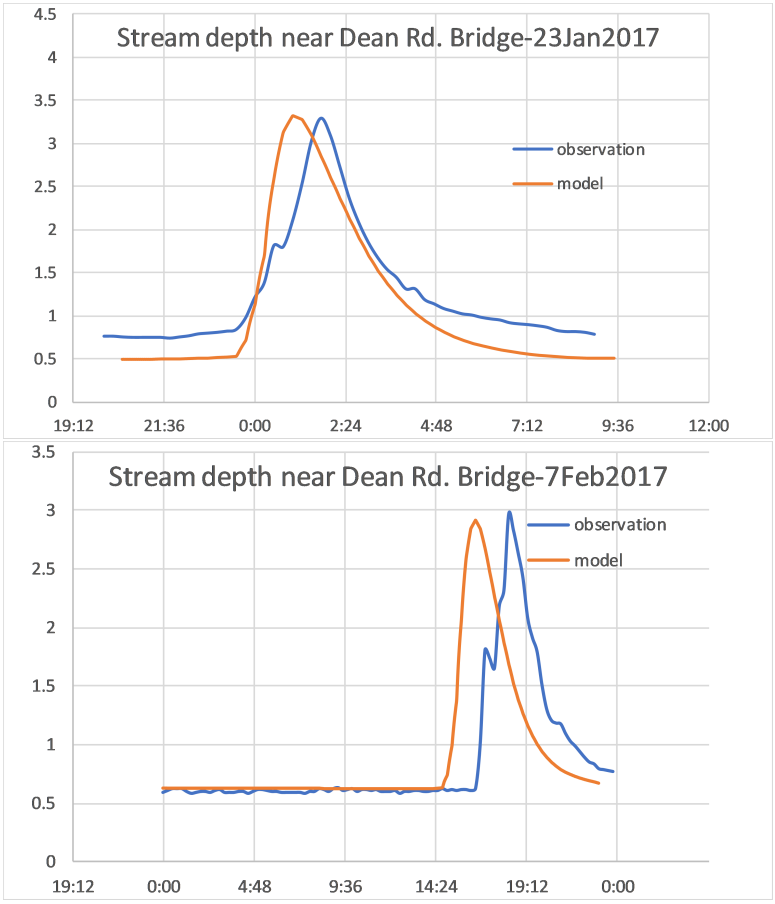


Figure 5.3: Stream depth hydrographs observed in Soapstone Branch and modeled with HEC-RAS 5 for two calibration rainfall events (1/23 and 2/7/2017) using outflows modeled by HEC-HMS.

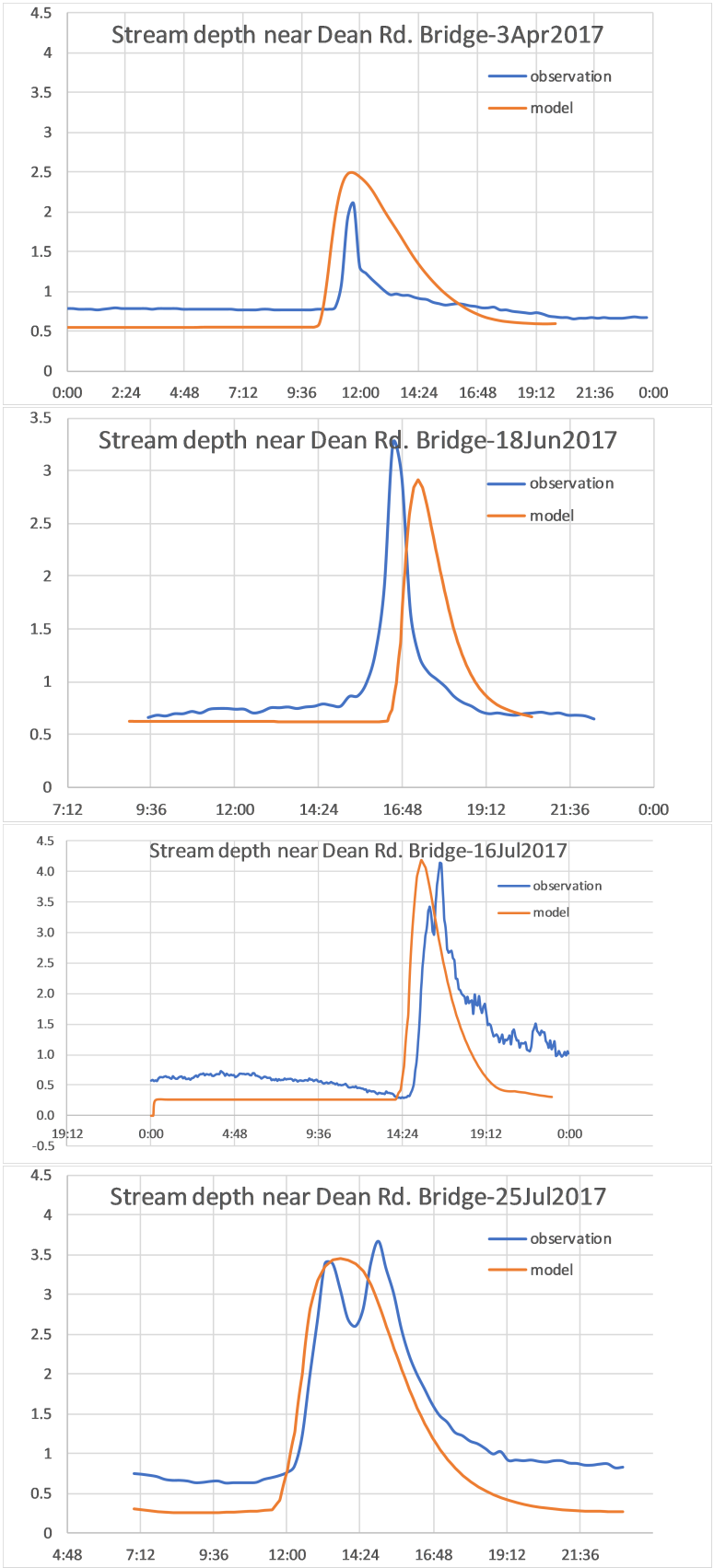


Figure 5.4: Stream depth hydrographs observed in Soapstone Branch and modeled with HEC-RAS 5 for four calibration rainfall events using outflows modeled by HEC-HMS.

An evaluation of the modeling results of depth hydrographs indicates that HEC-RAS was in general very accurate in representing the general changes in the stream stage during rainfall events. There is an offset on the observed and simulated peak flow time for some events, but the offset is most likely attributed to inaccuracy of the rainfall-runoff modeling using HEC-HMS such as the amount of rainfall abstraction.

After calibration was concluded, the largest discrepancy was 18%, with an average discrepancy under 10%.For the validation dataset, the greatest discrepancy in the peak depth observed in the calibration dataset was 25%,and the average discrepancy was 12%. Detailed results regarding the discrepancies in observed and modeled peak flow depth are presented in Table 5.1 . Given that the hydraulic model used results from another model to perform these analysis, it is considered that the modeling calibration and validation was successful.

Table 5.1: Results of peak flow depth discrepancy between calibration and validation datasets for rainfall events measured at Soapstone Branch Watershed. Depths measured and modeled upstream from the Dean Road Bridge site.

| **Calibration dataset** | | | |
|---|---|---|---|
| **Rain event date** | **Measured peak depth (ft.)** | **Modeled peak depth (ft.)** | **Peak depth discrepancy** |
| 16-Jun-16 | 3.4 | 2.8 | 17.6% |
| 9-Jul-16 | 3.6 | 3.5 | 2.8% |
| 3-Aug-16 | 2.4 | 2.7 | 14.9% |
| 13-Dec-16 | 1.8 | 1.6 | 10.9% |
| 1-Jan-17 | 3.2 | 3.0 | 6.3% |
| 7-Jan-17 | 2.5 | 2.3 | 8.0% |
| 21-Jan-17 | 1.6 | 1.6 | 4.5% |
| **Validation dataset** | | | |
| **Rain event date** | **Measured peak depth (ft.)** | **Modeled peak depth (ft.)** | **Peak depth discrepancy** |
| 23-Jan-17 | 3.3 | 3.3 | 0.0% |
| 7-Feb-17 | 3.0 | 2.9 | 3.3% |
| 3-Apr-17 | 2.2 | 2.5 | 13.6% |
| 9-May-17 | 2.8 | 2.2 | 21.4% |
| 18-Jun-17 | 2.8 | 3.3 | 17.9% |
| 16-Jul-17 | 4.1 | 4.1 | 0.0% |
| 25-Jul-17 | 3.0 | 3.7 | 25.4% |

## 5.2 Velocity and shear stress results at Soapstone Branch pre and post stream modification

One of the key objectives of this research is to assess whether a solution, other than bridge replacement, can be applied to solve the aggradation issue created by the sediment being transported by Soapstone Branch to Dean Road Bridge. The previous section demonstrated that the hydraulic modeling was successful in representing the flow conditions upstream from the bridge after calibration steps were concluded. This section will perform calculations associated with the shear stress in Soapstone Branch at this present condition, and compare with the shear stress values that would be anticipated with the changing the stream cross section near the bridge, also referred to as stream modification approach.

The proposed stream modification involves using a 2-ft deep, 20-ft wide trapezoidal cross section under the bridge. Upstream from the bridge the stream bed slope is 1%, and after the bridge the slope is 0.10%, with a total length of 240-ft of stream modified. The overarching idea is to facilitate sediment discharge across the bridge through steeper slope as Soapstone Branch approaches the crossing, and flatter slope downstream from the bridge. With this approach the intervention (stream modification) of channel cross sections in the Soapstone Branch would be limited to the vicinity of the Dean Road Bridge, as is shown in Figures 5.5, Figure 5.6 and Figure 5.7 .

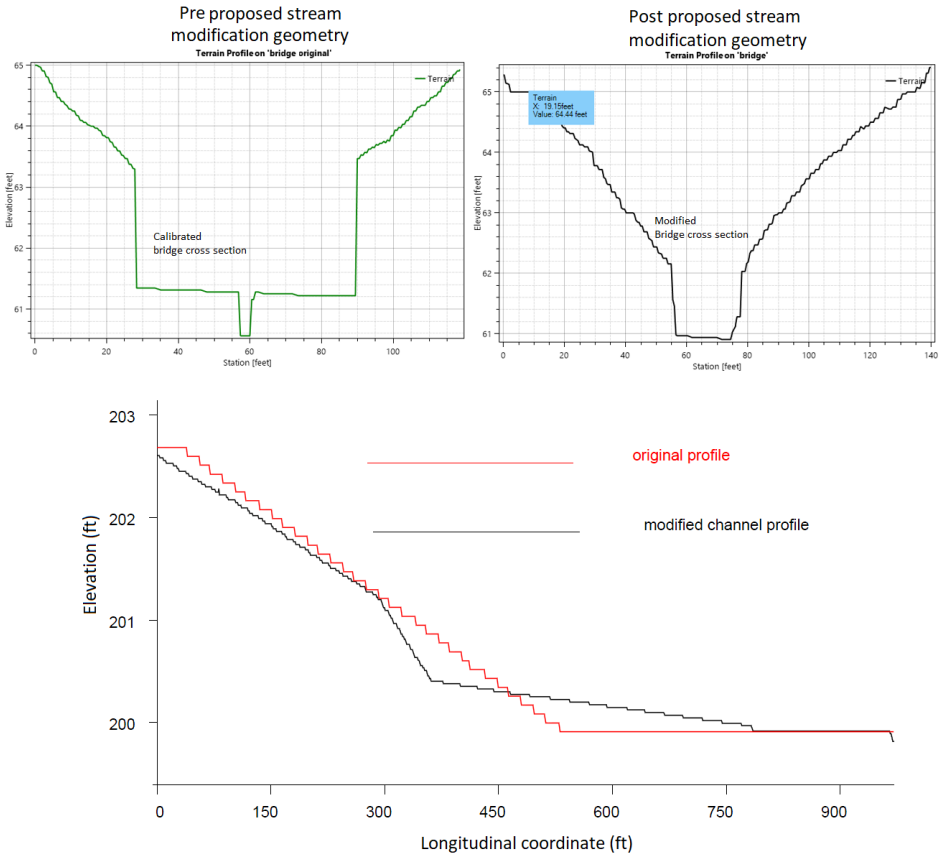


Figure 5.5: Soapstone Branch cross section under Dean Road Bridge prior to stream modification (top) and after (middle). The new stream profile (bottom) indicates a steeper profile near the Dean Rd. Bridge crossing.

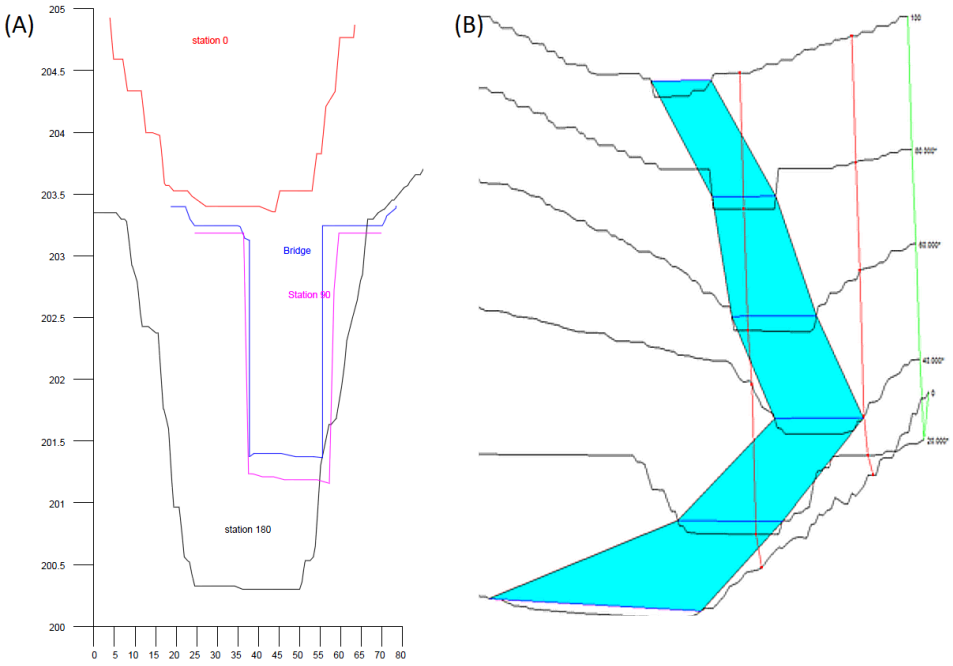


Figure 5.6: Cross sections of the modified Soapstone Branch (A), and Perspective of flow in Soapstone Branch in the post modification cross section near the bridge site, modeled by HEC-RAS 5 (B).

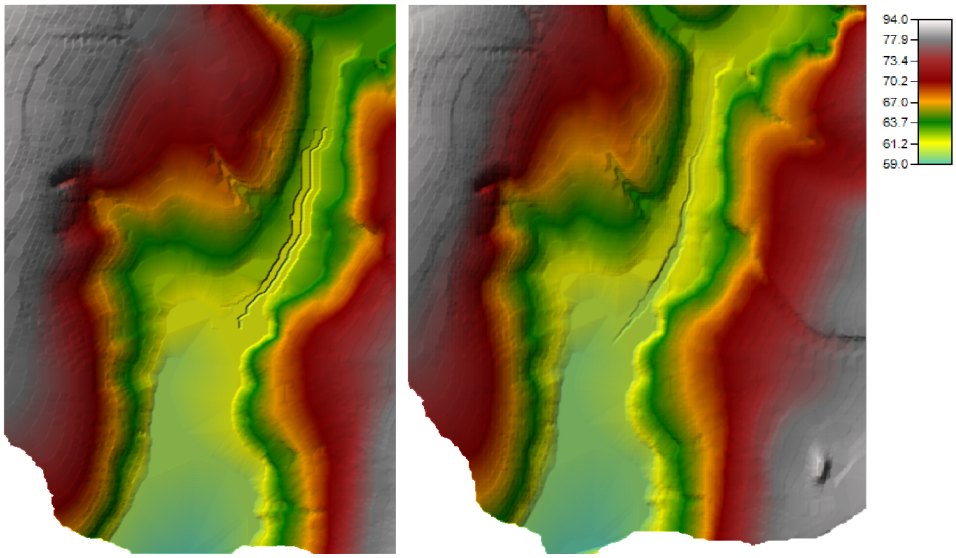


Figure 5.7: Changes in Soapstone Branch elevation map prior to stream modification (A) and after (B). A more streamlined pathway for sediment discharge is noticed after the modification.

In order to address whether aggradation issue can be mitigated with stream modification, it is necessary to ensure calculate shear stresses in the bottom of the stream for both pre and post-modification scenarios. It is important that the stream modification strategy to result in shear stress levels that are consistently higher than the level that are currently observed in Soapstone Branch. Figures 5.8 to 5.10 present a 2-D representation of the shear stress calculated with the model HEC-RAS 5 for one of the intense rain events (July 9, 2016) that was monitored in Soapstone Branch. Three different flow conditions are represented in these figures: peak flow conditions (Figure 5.8), 50% peak flow conditions (Figure 5.9) and base flow conditions (Figure 5.10), with current conditions represented with the letter (A), and letter (B) referring to post stream modification conditions.

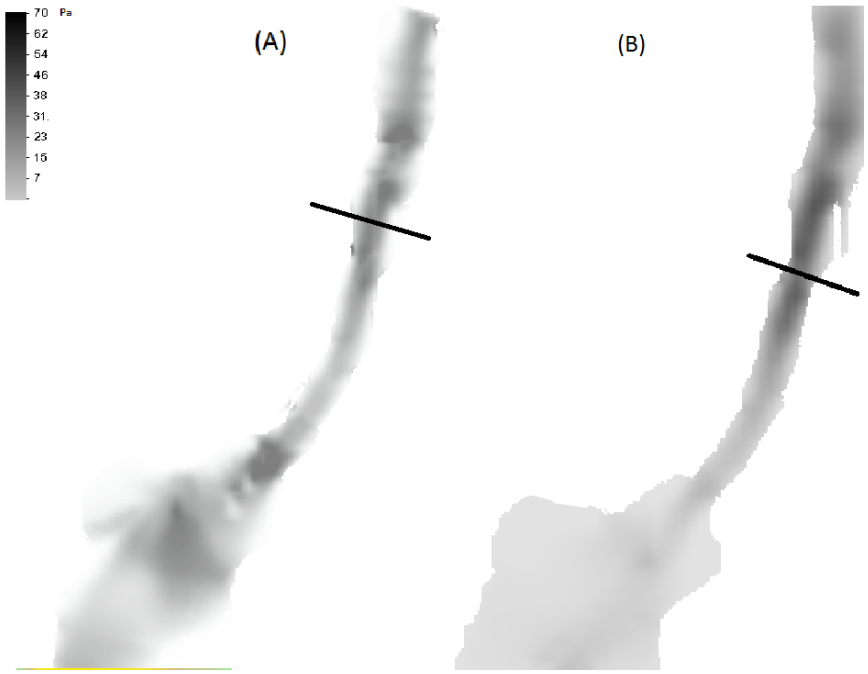


Figure 5.8: Shear stress results at Soapstone Branch in the peak flow for the 7/9/2016 event for pre-stream modification (A) and post stream modification scenarios (B). Results obtained with HEC-RAS 5.0 model.

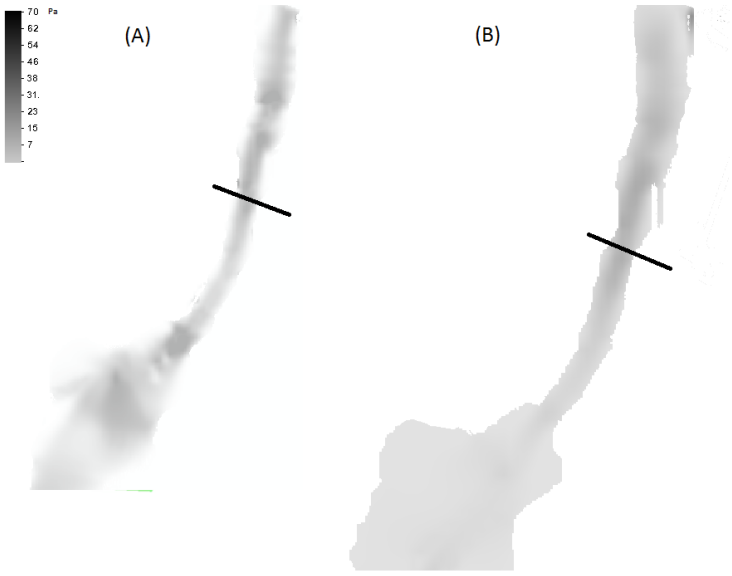


Figure 5.9: Shear Stress results at Soapstone Branch for 50% of the peak flow for the 7/9/2016 event for pre-stream modification (A) and post stream modification scenarios (B).

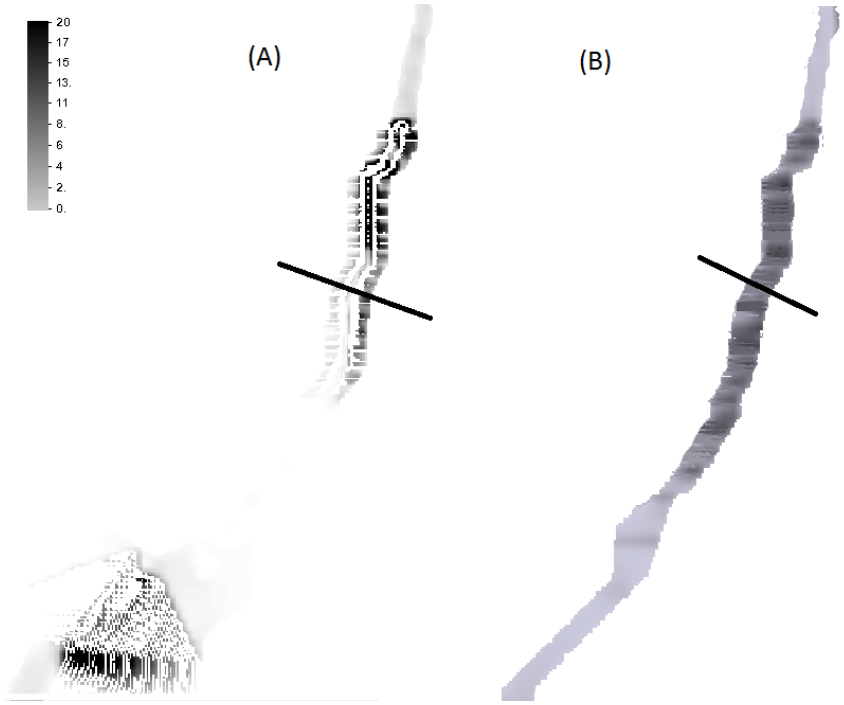


Figure 5.10: Shear Stress results at Soapstone Branch for the base flow conditions (1.4 cfs) for pre-stream modification (A) and post stream modification scenarios (B).

An evaluation of the simulation results presented in Figures 5.8 to 5.10 allows to determine that the stream modification alternative increases shear stresses in all three stages. This is

the case of the shear stress at the peak flow conditions in the neighborhood of Dean Road Bridge, marked with a magenta-colored line. Most importantly, shear stress levels are higher for the base flow conditions (1.4 cfs), which indicate a better capability of the changed stream geometry to allow the passage of sediment across the bridge cross section, even with low flow conditions.

### 5.3 Result comparison between HEC-RAS and SRH-2D

While shear stress is a fundamental variable to be studied in this evaluation of sediment motion near Dean Road Bridge, another important assessment would be the actual calculation of sediment motion near the bridge crossing for both pre and post stream modification scenarios. There is a practical difficulty, however, posed by the model used thus far. HEC-RAS 5 is still unable to simulate sediment motion in streams. This research has thus opted to adopt another entirely different model, SRH-2D, developed by the US Bureau of Reclamation, to perform 2-D river flow modeling alongside with sediment motion.

However, prior to start these calculations, it was first necessary to ensure that SRH-2D model results are consistent with the calculated results obtained from HEC-RAS. The mesh generation process for SRH-2D, described in Chapter 4, yielded a mesh size that was consistent in dimensions with the HEC-RAS 5 model. Also, the inflow information and boundary conditions adopted in SRH-2D matched the same ones used in the HEC-RAS model. Yet, such assessment is necessary to ensure the validity of calculations. The comparison indicated that the model results were very consistent. As is shown in Figure 5.11, for the 7/9/2016 flood event, depth and velocity predicted by both models near the bridge site are very much in agreement.

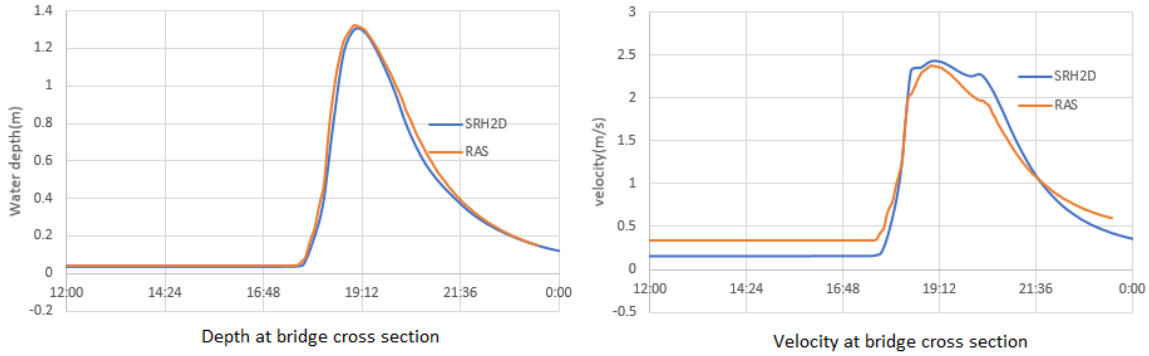


Figure 5.11: Comparison between the stream flow depth and velocity calculated at the Dean Road Bridge cross section for the 7/9/2016 rain event by HEC-RAS 5 model and SRH-2D model.

Shear stress results for the post stream modification obtained between HEC-RAS and SRH-2D indicate that shear stress levels are in the same range. Shear predictions from SRH-2D tend to be higher downstream from the bridge when compared to HEC-RAS. This can be viewed in the results for the 7/9/2016 flood event presented in Figure 5.12 (100% of the peak flow), Figure 5.13 (50% of the peak flow) and in base flow conditions, shown in Figure 5.14. Such consistency enabled the continuation of modeling assessments with focus on sediments to using the SRH-2D model, which is the focus of the next section.

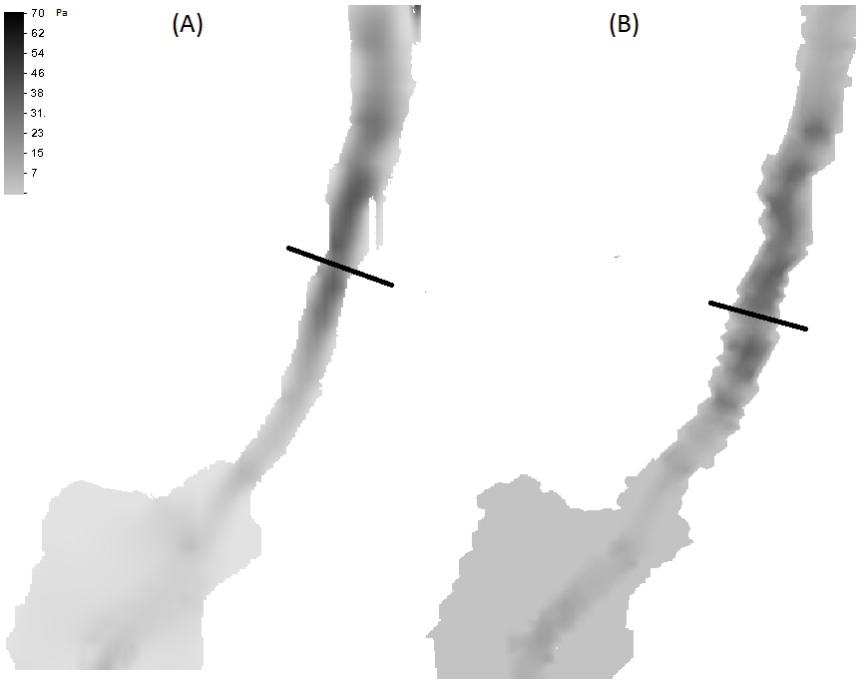


Figure 5.12: Comparison between the shear stress in Soapstone Branch for the 7/9/2016 rain event, at the peak flow conditions, by (A) HEC-RAS 5 model and (B) SRH-2D model.

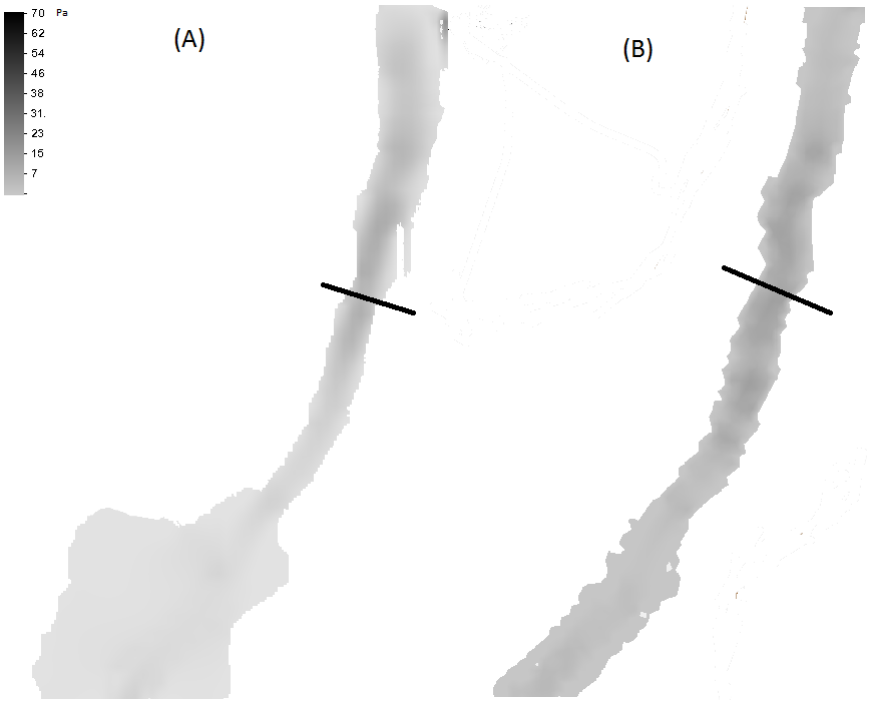


Figure 5.13: Comparison between the shear stress in Soapstone Branch for the 7/9/2016 rain event, at half of the peak flow conditions, by (A) HEC-RAS 5 model and (B) SRH-2D model.

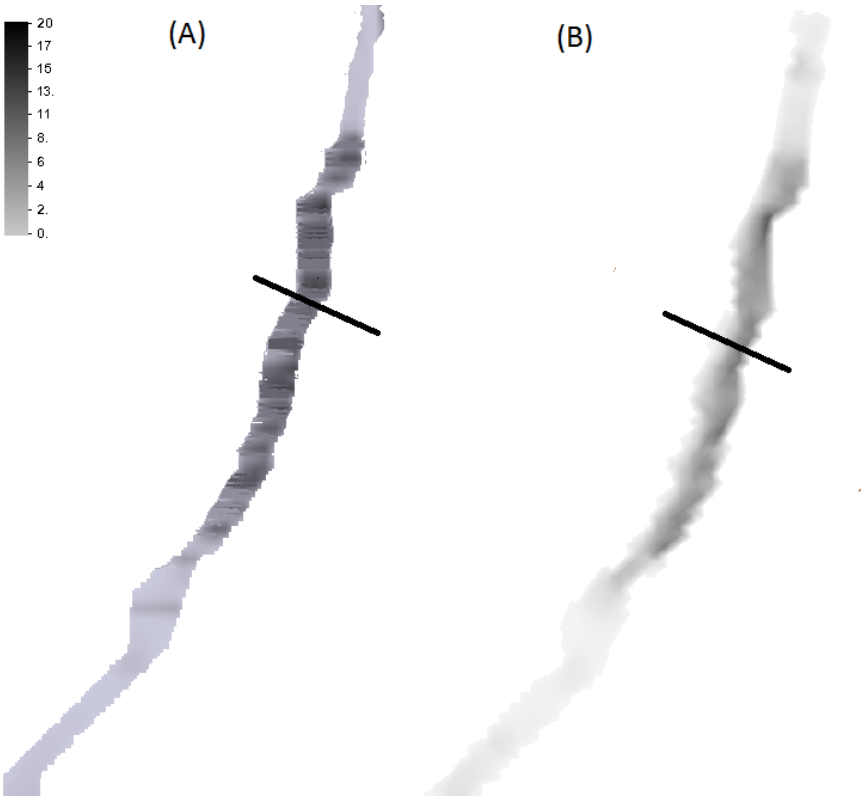


Figure 5.14: Comparison between the shear stress in Soapstone Branch for the 7/9/2016 rain event, at base flow conditions (1.4 cfs), by (A) HEC-RAS 5 model and (B) SRH-2D model.

## 5.4 Calculations of sediment transport in Soapstone Branch by SRH-2D model

All SRH-2D simulations presented in the previous subsection assumed stable stream beds, which is not the case when sediment transport occurs in the stream. To enable the calculation of sediment discharges, SRH-2D requires information of sediment loading in the upstream boundary condition.

During the field data collection phase, samples of stream flow were collected for different rain events. This enabled to correlate stream turbidity along with values of total suspended solids concentration (TSS, expressed in mg/L), each associated with observed stream depths. With stream depth measurements and flow rate results of numerical modeling, it was possible to correlate the observed TSS with varying stream flow values. From this correlation, a TSS-flow expression was developed, based on the field observed values. Values shown in Figure 5.15 indicate that the assumed TSS-flow expression is more conservative than the observed

TSS-flow values. The idea is that such correlation could represent the conditions of sediment inflow in Soapstone Branch that are more intense than the ones observed.

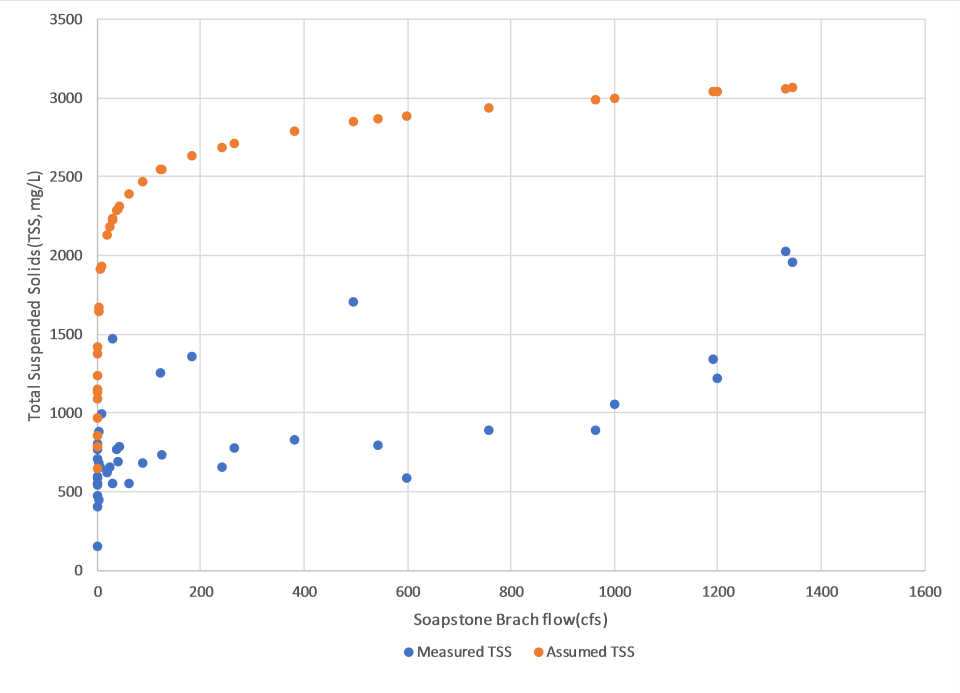


Figure 5.15: Sediment discharge curve assumed for Soapstone Branch used in the simulation results, derived from the TSS-flow relationship measurements in this research and used in SRH-2D modeling.

Through appropriate conversion, and assuming sediment density as 2,650 $kg/m^3$, another relationship expressing sediment volumetric flow rate in terms of the stream flow rate was derived for Soapstone Branch. This expression, presented in Figure 5.16, is needed by SRH-2D to perform sediment concentration. Another information that is needed is the particle size distribution for the site, which is presented in Figure 5.17. There is a degree of estimation in sediment discharge given that direct measurement of this parameter was not included in the original project scope.

The assessment of sediment aggradation process was based on a 30.5-day long simulation performed in SRH-2D. This was an hypothetical scenario, not resembling a particular set of rain events. It was meant to study effect of base flows in sediment transport in Soapstone Branch as

well a severe flood, as it would be predicted by SRH-2D. This simulation had different stages, with separate goals:

- First, it was intended to consider an initial 30 days of the simulation assuming base flow conditions at 1.4 cfs (0.040 $m3/s$), associated with low sediment inflows. The goal of this part of the simulation was to verify whether in extended low flow conditions if there would be a long-term tendency of sediment build up near the bridge site, according to the SRH-2D simulation results.

- After this 30-day period, it was assumed that Soapstone Branch would undergo 12-hour of high flow condition associated with a rain event that creates a 25-year return period flow. The rain event that was recorded in July 9, 2016 created a peak flow of 37 m3/s, or 1,307 cfs. According to Streamstats program (Ries III et al., 2008), this event has an intensity similar to an event with a 25-year return period, as indicated in Table 5.2. The goal of this second stage was to assess how sediment distribution would change as result of a large rain event occurring in Soapstone Branch watershed.

- Finally, another 30-day period of base flows was simulated to evaluate the tendency of the stream to recover from the morphologic changes created by the intense rain event.

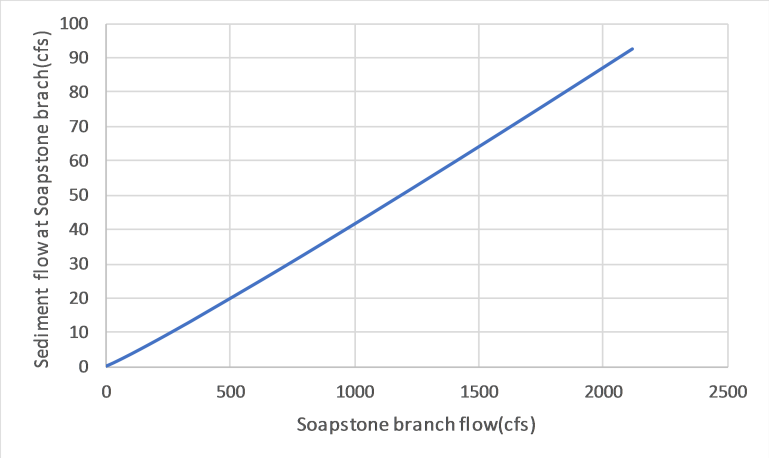


Figure 5.16: Sediment discharge curve assumed for Soapstone Branch that was used in the SRH-2D simulation, derived from the TSS-flow relationship measurements.

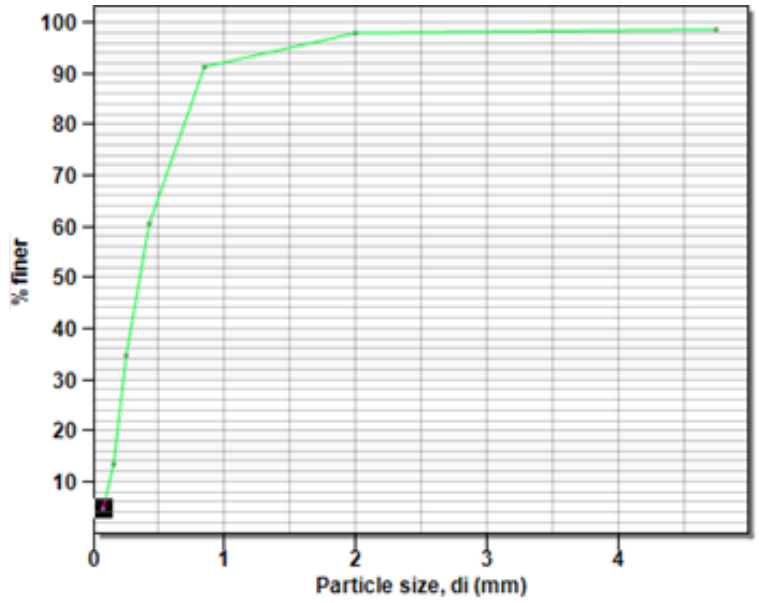


Figure 5.17: Particle size distribution representative of sediment transported in Soapstone Branch used in SRH-2D modeling.

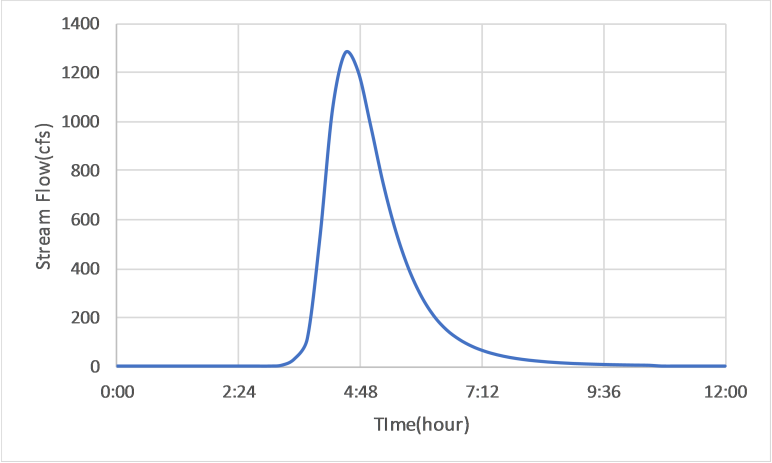


Figure 5.18: Inflow hydrograph for the 7/9/2016 rain event, with an intensity similar to a 25-yr return period event, and used for the sediment transport assessment with SRH-2D. From 10 to 12 hours, not shown in the graph, flows are near base flow conditions.

Table 5.2: Return period of Soapstone Branch according to Streamstats (Ries III et al., 2008). The 25-year flood is similar to the intensity recorded in the July 9,2016 rain event

PII: Prediction Interval-Lower, Plu: Prediction Interval-Upper, SEp: Standard Error of Prediction, SE: Standard Error (other -- see report)

| Statistic | Value | Unit | SE | SEp | Equiv. Yrs. |
|---|---|---|---|---|---|
| 1.5 Year Peak Flood | 302 | ft^3/s | 37 | 37 | 4 |
| 2 Year Peak Flood | 394 | ft^3/s | 33 | 33 | 5 |
| 5 Year Peak Flood | 710 | ft^3/s | 26 | 26 | 11 |
| 10 Year Peak Flood | 963 | ft^3/s | 24 | 24 | 18 |
| 25 Year Peak Flood | 1330 | ft^3/s | 25 | 25 | 26 |
| 50 Year Peak Flood | 1640 | ft^3/s | 27 | 27 | 28 |
| 100 Year Peak Flood | 1980 | ft^3/s | 29 | 29 | 28 |
| 200 Year Peak Flood | 2340 | ft^3/s | 33 | 33 | 27 |
| 500 Year Peak Flood | 2860 | ft^3/s | 37 | 37 | 26 |

The initial conditions of the simulation (T=0 day), expressed in terms of the stream bed elevation, is presented in Figure 5.19 A. Following this initial condition, 30 days of a based flow was assumed to occur. Figure 5.19B presents the same region after 30 days of the base flow (1.4 cfs). The only significant change observed in these days was due to the increased flow velocity downstream from the modified stream near the bridge. This higher velocity resulted in a ripple pattern aligned with the flow direction downstream from the modified stream. But there is no systematic increase in stream bed elevation near the bridge crossing. Figures 5.19C and 5.19D present results 4 hours and 8 hours into the intense rain event that occurs in the simulation after the 30-day base flow period. Results indicate that during the 12 hours very significant changes in stream bottom elevation on Soapstone Branch can occur, but not influence the locations near the bridge or the modified stream.

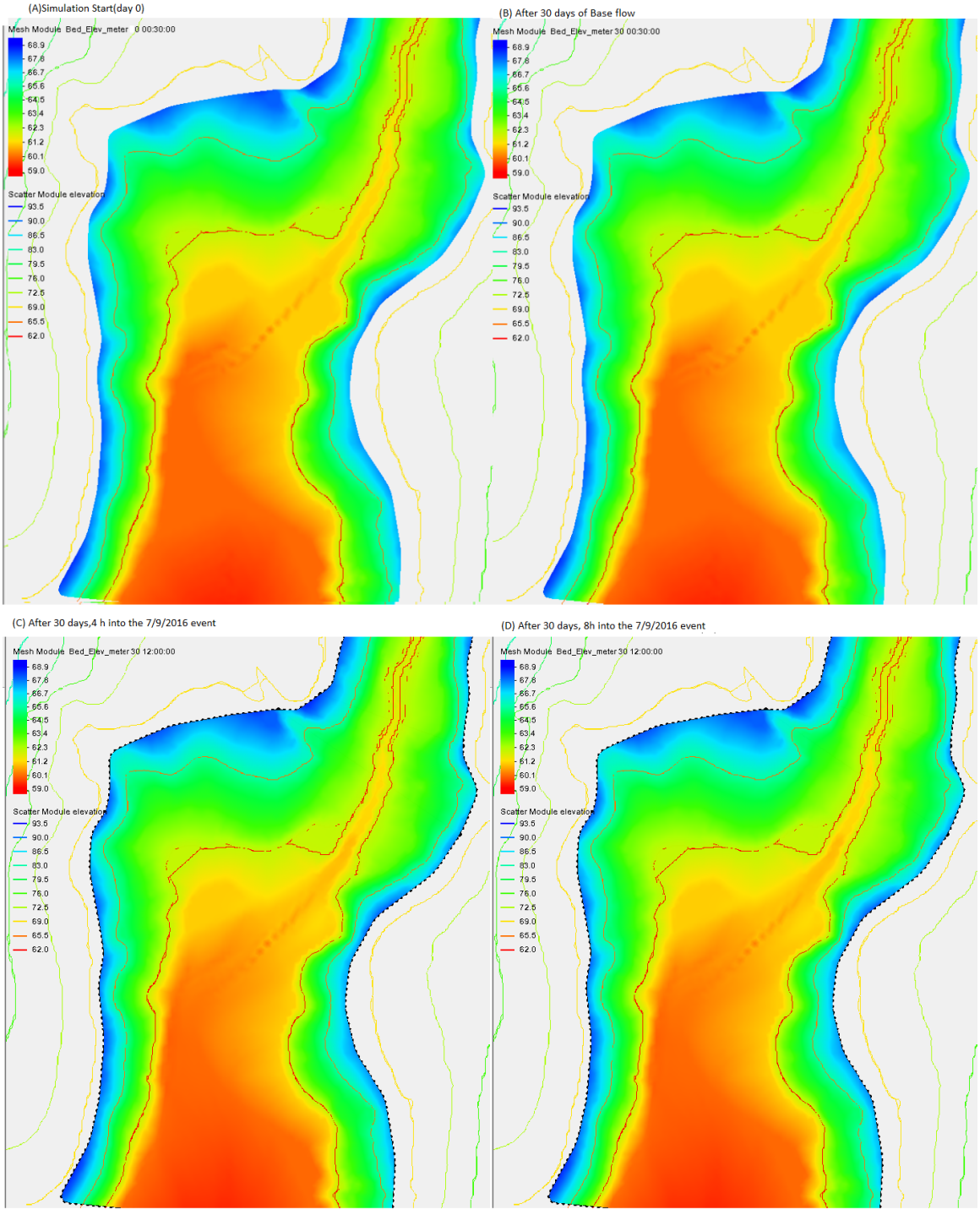


(c) day30h8 (d) day30h12

Figure 5.19: Predicted streambed elevations yielded by SRH-2D model for a 30.5 day long simulation at various times, from the beginning of the simulation, into 30 days of base flow, and then in two instants after a 12-hour long intense rain event that happened in 7/9/2016.

Figures 5.20 and 5.21 present the incremental changes in bed elevation observed for the 30-day period of base flow or the 12-hour long intense hydrograph, respectively. Values correspond to decreased depth (scour) and red to aggradation. These results show development of sand dunes upstream from the bridge, with stream bed scour to 0.40 m and aggradation to 0.15 m in the stream bed channel over the 30-day period. After the large rain event, there is some aggradation upstream from the stream modification site, typically under 15 cm. Downstream from the bridge site, the steeper slope created conditions for sediment flushing, and minor scour (under 9 cm) resulted from the large rain event. Following this intense rain event, the model results of an additional 30-day period of base flow, shown in Figure 5.22, show that scour holes are gradually filling up, and aggradation levels are preserved, but no aggradation in the bridge is observed.

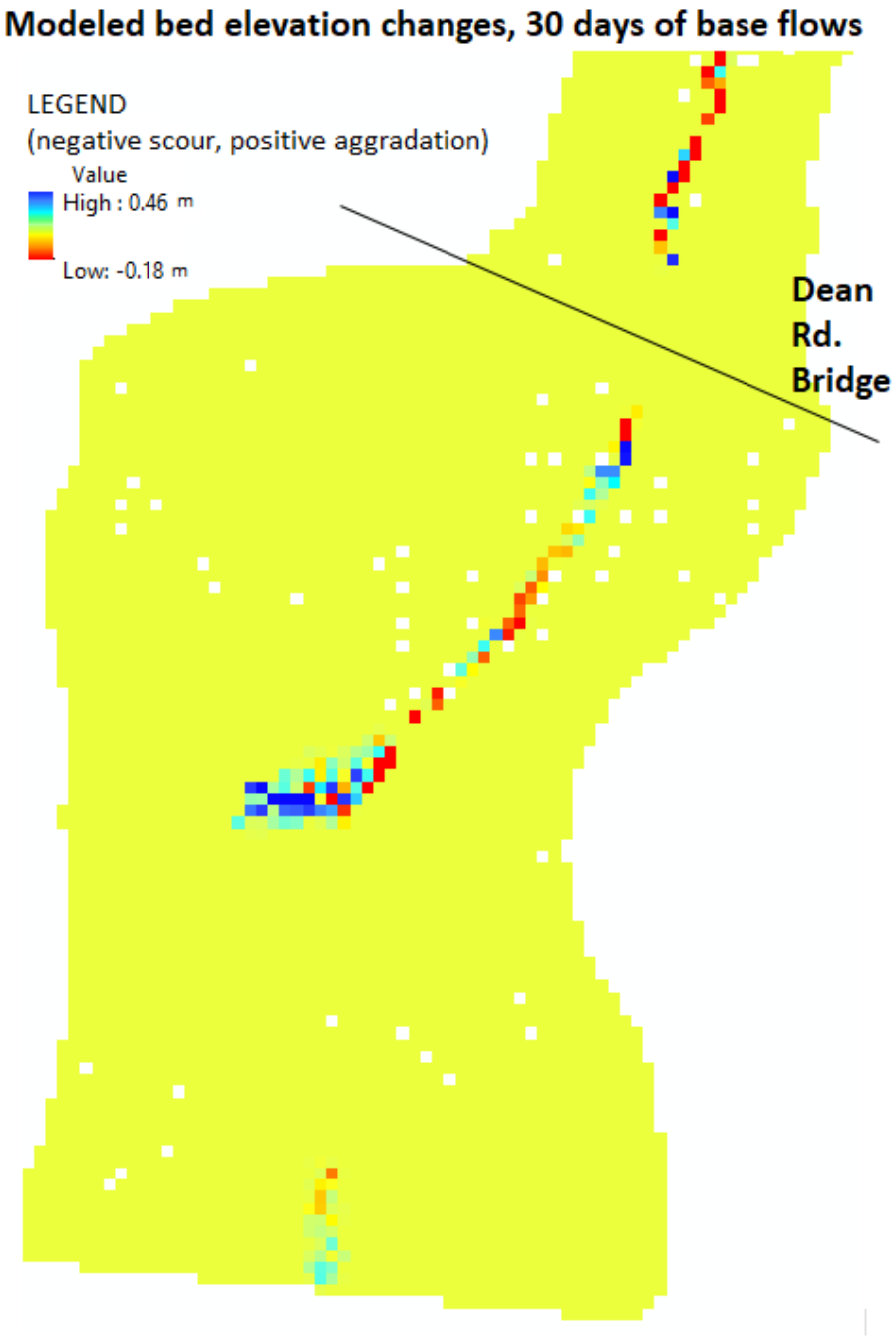


Figure 5.20: Predicted incremental changes for Soapstone Branch during 30 days of base flow conditions. Blue is aggradation, red is scour with respect to original elevation (T=0 days).

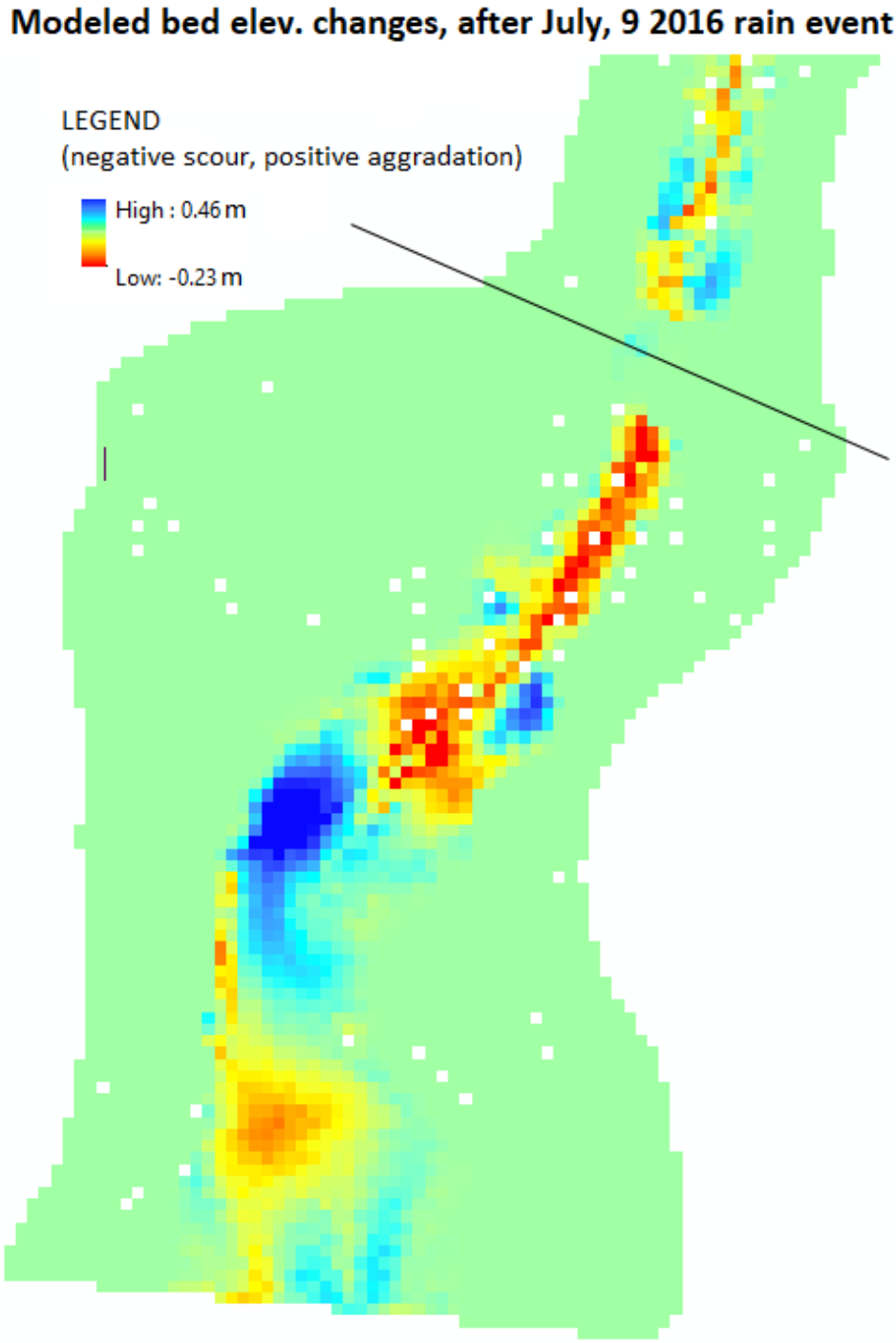


Figure 5.21: Predicted incremental changes for Soapstone Branch during a 12-h period after the 7/9/2016 rain event. Blue correspond to aggradation, red is scour with respect to original elevation (T=0 days).

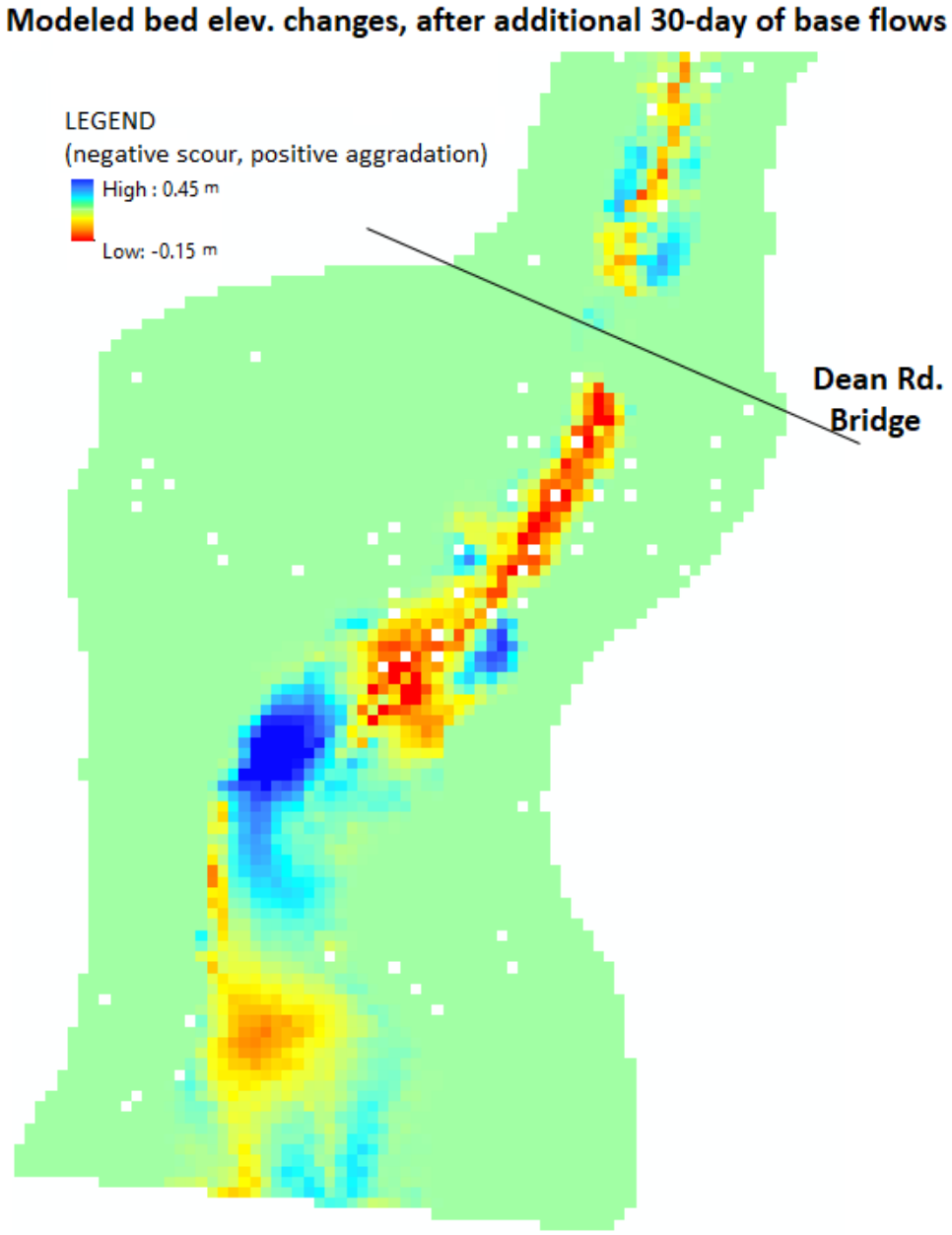


Figure 5.22: Predicted bed elevation changes for Soapstone Branch after the 7/9/2016 rain event and after another 30 days of base flow. Red correspond to aggradation, green is scour with respect to original elevation (T=0 days).

Figure 5.23 presents the results from 3 points selected downstream from the stream modification region to show the evolution of the elevation changes during the 12 hours of the intense hydrographs. Changes in points A, B and C indicate that scour and aggradation can occur simultaneously, and that most of the observed changes take place as the flow intensity in the

stream increased to a maximum, from 6 to 10 hours of the hyetograph.

In summary, these results indicate that the stream modification can be an effective strategy in pushing sediments from the location where the bridge is, creating a region with minor scour downstream from the modified stream. The minor aggradation upstream from the bridge occurring during base flows is likely to be removed with the tendency for scour during base flow conditions. Provided that the sources for sediment upstream from Soapstone Branch can be reduced or mostly eliminated, a solution based on stream modification could be successful.

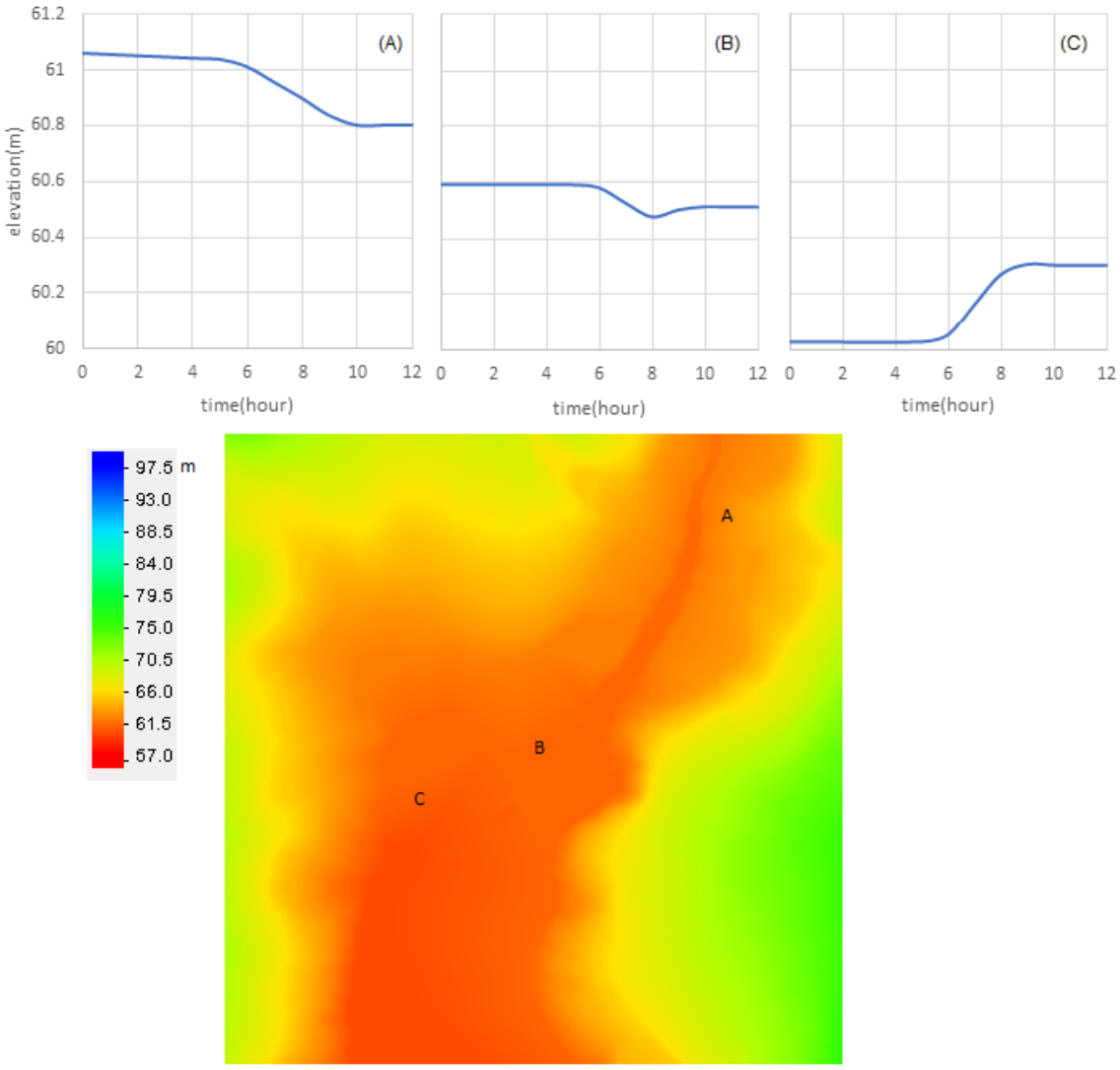


Figure 5.23: Evolution of stream bed elevation for points A, B and C located downstream from the stream modification region of Soapstone Branch.

## 5.5 Latest changes in the research site and related numerical modeling

During September 2018 the research team returned to Soapstone Branch watershed one last time to retrieve the sensors used in the investigation and determined that a temporary steel bridge has been placed immediately downstream from the existing Dean Road Bridge. This bridge was placed at a higher elevation, following a sequence of rain events that damaged further the old Dean Road Bridge over Soapstone Branch. This temporary bridge, constructed in a steel, is presented in Figure 5.24.

Figure 5.24: newbridge

It was determined that the bridge is supported directly on the two embankments that were constructed to a higher grade elevation, enabling the structure to avoid immediate overtopping. The embankments are filled with riprap to eliminate the erosion created by the Soapstone Branch peak flows . These embankments create a contraction to Soapstone Branch geometry that was not considered in previous modeling efforts. Thus a new group of numerical simulations were added to this research effort, also using SRH-2D.

This new SRH-2D model was built with field estimates of the new bridge geometry. The bed elevation of the channel bank right downstream of the channel is raised 8ft higher than the original elevation and was set to be unerodable. The bottom width of the main channel was assumed as 30-ft wide, and side slopes were assumed as 1V:2H. The inflow conditions assumed for the 25 year rain event. The simulation result shows that there may be aggradation

at east side of the channel and a small amount of scour the west side of the channel. Following a 25-year return period rain event, this aggradation may amount to 15 cm, with a corresponding scour of 2 cm, as is illustrated in Figure 5.25.

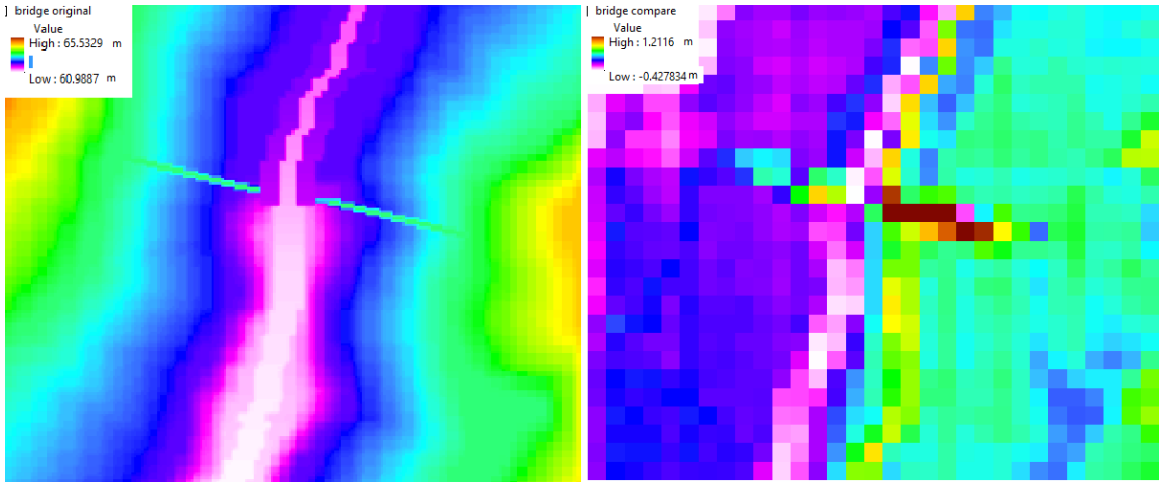


Figure 5.25: New terrain elevation (estimated) near Dean Road bridge and resulting change in stream level due to scour (negative) and aggradation (positive) resulting from the temporary steel bridge construction.

Signs of this aggradation process are actually already observable in that there is an accumulation of sediment in the east bank, downstream from the bridge, as is shown in Figure 5.26. This bank is approximately already 1 ft above the water level in the stream. In Figure 5.26 this bank presents a breach, which is caused by the discharge of stormwater drainage flows from the east part of Dean Road. To some extent, this outcome is expected given that a needed change in the stream bed slope, to help flush sediments away from Dean Road bridge, was not performed with the construction of this temporary bridge.

This actually, is another source of potential problems in this temporary steel bridge solution. There are clear signs of erosion in the bridge approaches, particularly the one in the east end of the bridge. Moreover, a culvert discharging stormwater flow from Dean Road without proper energy dissipation is eroding the newly built approaches for the temporary steel bridge, as is shown in Figure 5.27. Without immediate intervention in the bridge this erosion process will continue and may compromise the integrity of the bridge and lead to a catastrophic failure.

Figure 5.26: Aggradation signs on the east side of Soapstone Branch, downstream from temporary steel bridge

Figure 5.27: Surface erosion in the eastern embankment and erosion created by stormwater flows from Dean Road, creating slope failures immediately upstream from the temporary steel bridge.

# Chapter 6

## Conclusions and recommendations for future studies

This research was motivated by a serious aggradation problem occurring on the Dean Road bridge in Dale County, as it crosses Soapstone Branch catchment, a tributary of Little Choctawhatchee River. Historical aerial imageries of the catchment revealed increasing deforestation occurring in a short period of time (2011 to 2015), some of which near or at the stream banks. The research involved the development of a field investigation, use of hydrological modeling tools and hydraulic modeling tools. The goals involved the quantification of changes in sediment yield in the past years, as well to assess whether a stream modification strategy could result in a sustainable means for sediment discharge in the cross section.

Hydraulic models were built on Soapstone Branch near Dean Road Bridge. Based on the stream flows calculated from the hydrological model, the main goal was to compute shear stress near the bridge crossing at current conditions and after a stream modification strategy. The stream modification intended to facilitate sediment discharge through increasing the stream bed slope as Soapstone Branch approached Dean Road Bridge.

The first step needed to achieve this goal was to perform a calibration of the hydraulic model, which involved choosing an adequate Manning roughness factor. However, flow conditions near the bridge are specially challenging due to varying amount of sediment accumulated under the bridge during a flooding event. The varying flows result in a partial clearing of the sediment under the bridge during a rain event, leading to pressurized flows under the bridge. In addition, overtopping may also occur if the flow rates are large. Various geometry surrogates to represent the behavior of the observed depth-discharge for a variety of rain events. A geometry was found that successfully represented the head discharge near the bridge site, enabling a study on shear stresses at other areas near Dean Road Bridge.

The numerical simulations to investigate shear stresses at Soapstone Branch compared the existing condition and the conditions after the stream modification was introduced. It was

shown that the proposed stream modification yielded consistently larger values of shear stress in the stream near the bridge site. This indicates that this alternative would facilitate the transport of sediment near the bridge site, mitigating the aggradation process.

One shortcoming of this stage of the research was the inability of the hydraulic model (HEC-RAS 5) to simulate sediment transport in this two-dimensional simulation framework. To overcome this issue another hydraulic model, SRH-2D, was used in this work. Comparisons were made between HEC-RAS 5 and SRH-2D results in terms of flow depth and velocity, and modeling results were shown to be very consistent with each other. Thus SRH-2D shear stress predictions were generated and results of simulated shear stress from both models compared fairly well. The last stage of the hydraulic modeling process involved using SRH-2D model for an extended (30.5-day long) simulation that represented one month of base flows followed by an intense rain event. These results showed that no significant aggradation occurred near the bridge site during the initial 30 days (aggradation under 15 cm or 0.5 ft.). The intense rain event results in minor aggradation upstream from the bridge (typically under 20 cm or 0.7 ft.) and minor scour downstream (less than 9 cm or 3.5 in.). This indicates that the proposed alternative can be sustainable, avoiding the need of channel dredging that is currently in place. This stream modification strategy also is likely to be significantly less expensive than an alternative involving the replacement of Dean Road Bridge.

The continuation of this research could involve the following steps:

- Monitoring of other bridge or culvert crossings in the State of Alabama that are experiencing similar aggradation issues, and apply the methodology used in this study to evaluate alternatives to solve the aggradation issue.

- Development of the 2nd stage of research in rivers downstream from Soapstone Branch to determine if the aggradation issues created in the nearby watersheds are impacting these bridge conveyance capacity.

- Improve the methodology used in the present research by exploring other alternatives to perform hydrological studies and sediment yield analysis. With this methodology, map

bridge crossings across the State of Alabama that are more at risk of being impacted by aggradation processes.

- Perform a detailed analysis of the role of streambank failure mechanism in the amount of sediment generation in Soapstone Branch.

References

Aquaveo, L. (2017). Mesh editing. sms 12.2 tutorials.

Aricò, C. and Tucciarelli, T. (2008). Diffusive modeling of aggradation and degradation in artificial channels. *Journal of Hydraulic Engineering*, 134(8):1079–1088.

Arneson, L., Zevenbergen, L., Lagasse, P., and Clopper, P. (2012). *Evaluating Scour at Bridges*. Federal Highway Administration (FHWA).

Briaud, J.-L. (2004). *Pier and contraction scour in cohesive soils*, volume 516. Transportation Research Board.

Brown, G. and Krygier, J. (1971). Clear-cut logging and sediment production in the oregon coast range. *Water Resources Research*, 7(5):1189–1198.

Brunner, G. (2016). River analysis system. 2d modeling user's manual. Technical Report CPD-68A, US Army Corps of Engineers.

Brunner, G. and Gibson, S. (2005). Sediment transport modeling in hec ras. In *Impacts of Global Climate Change*, pages 1–12. Hydrologic Engineering Center, U.S. Army Corps of Engineers.

Brunner, G. W. (2010). *HEC-RAS River Analysis System: Hydraulic Reference Manual*. US Army Corps of Engineers, Institute for Water Resources, Hydrologic Engineering Center.

Castro, J. and Reckendorf, F. (1995). *Effects of sediment on the aquatic environment: potential NRCS actions to improve aquatic habitat*. US Department of Agriculture, Soil Conservation Service.

Cunge, J., Holly, F., and Verwey, M. (1980). *Practical Aspects Computational River Hydraulics*. Pitman Advanced Publishing Program.

ESRI, E. S. R. I. (2011). *ArcGIS Desktop: Release 10.* Redlands, CA.

Farnsworth, R. K. and Thompson, E. S. (1983). *Mean monthly, seasonal, and annual pan evaporation for the United States*. US Department of Commerce, National Oceanic and Atmospheric Administration, National Weather Service.

FHWA (2018). *National Bridge Inventory*. URL https://www.fhwa.dot.gov/bridge/nbi.cfm.

Ghimire, G. R. and DeVantier, B. A. (2016). Sediment modeling to develop a deposition prediction model at the olmsted locks and dam area. In *2016 ASCE EWRI World Environmental and Water Resources Congress*, pages 410–420.

Glaister, P. (1988). Approximate riemann solutions for shallow water equations. *Journal of Hydraulic Research*, 26(3):293–306.

Harbor, J. (1999). Engineering geomorphology at the cutting edge of land disturbance: erosion and sediment control on construction sites. *Geomorphology*, 31(1-4):247–263.

Hogan, S. (2015). Advancements in two-dimensional floodplain modeling with srh-2d.

Johnson, P., Hey, R., Horst, M., and Hess, A. (2001). Aggradation at bridges. *Journal of Hydraulic Engineering*, 127(2):154–157.

Lagasse, P., Clopper, P., Pagan-Ortiz, J., Zevenbergen, L., Arneson, L., Schall, J., and Girard, L. (2009). Bridge scour and stream instability countermeasures: experience, selection, and design guidance: Volume 1. Technical report, National Highway Institute.

Lagasse, P., Zevenbergen, L., Spitz, W., and Arneson, L. (2012). Stream stability at highway structures. Technical report, Federal Highway Administration.

Lai, Y. G. (2008). Srh-2d version 2: Theory and user's manual. *Sedimentation and River Hydraulics–Two-Dimensional River Flow Modeling, US Department of Interior, Bureau of Reclamation, November*.

Patankar, S. (1980). *Numerical Heat Transfer and Fluid Flow*. CRC press.

Richardson, E., Simons, D., and Lagasse, P. (2001). River engineering for highway encroachments-highways in the river environment. Technical Report Hydraulic Series No. 6, Publication NHI-01–004, Federal Highway Administration , Washington, DC.

Ries III, K., Guthrie, J., Rea, A., Steeves, P., and Stewart, D. W. (2008). Streamstats: A water resources web application. *US Geological Survey Fact Sheet*, 3067(6).

Tamang, S. (2017). Quantifying flow and sediment yield of an ungauged catchment using a combination of continuous soil moisture accounting and event-based curve number method. Master's thesis, Auburn University.

Tamang, S., Song, W., Fang, X., Vasconcelos, J., and Anderson, J. (2018). Framework for quantifying flow and sediment yield to diagnose and solve the aggradation problem of an ungauged catchment. *Proceedings of the International Association of Hydrological Sciences*, 379:131.

Yang, C. (1996). *Sediment transport: theory and practice*. McGraw-hill New York.

Zhang, H. and Kahawita, R. (1987). Nonlinear model for aggradation in alluvial channels. *Journal of Hydraulic Engineering*, 113(3):353–368.

# Appendix A

## DEM Changing Details

This section presents the details for the DEM editing procedures used in this research. The detailed process is presented in four figures and a sequence of steps that are present in this appendix. A flowchart presented in Figure A outlines the entire procedure, however other scripts are also needed and are covered in the flowcharts presented in Figures A, A, and A.

**Main DEM editing procedure**

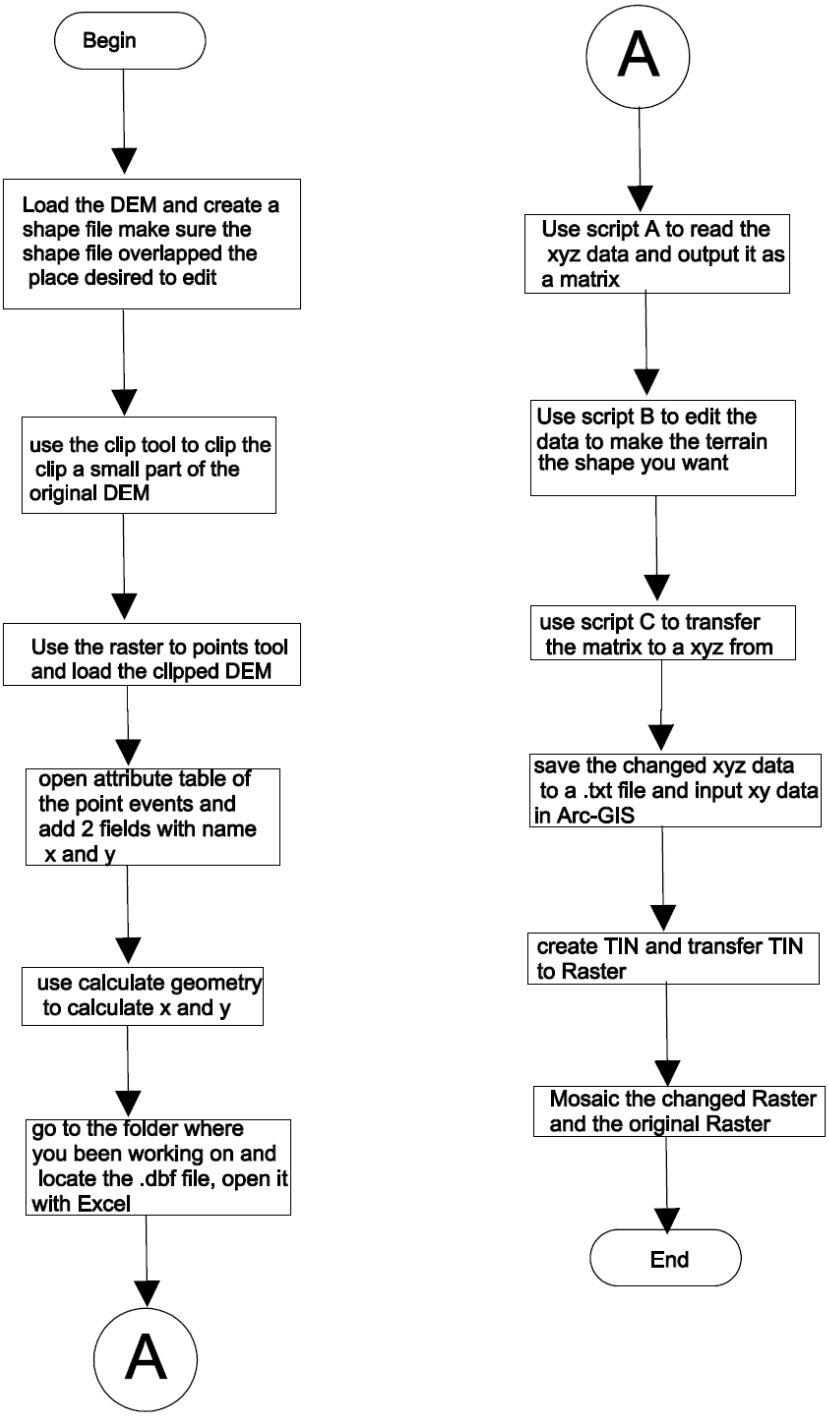


Figure A.1: General Flow Chart

Detailed steps:

1. Load DEM in ESRI ArcGIS and create a new polygon shape file

2. Edit the shape file to make the polygon overlap the place desired

3. Use Clip tool in Data Management tool box to clip the DEM to small parts of the original DEM

4. Select one DEM clip and search for the Raster to Point tool in tool box

5. Search for Extract Multi Values to Points and input your DEM and point shape file

6. Open Attribute Tables in the Table of Contents and go to table options

7. Select add field and add two files using the name of ”x” and ”y” with double precision

8. Right click on the top of the field and select calculate geometry. Select the correct coordinates that needs the calculation.

9. Go to the folder you been working on and find a .dbf file with the same name as your point shape file

10. Copy all the data in that .dbf file to a new MS Excel sheet. If the data is less than 10000 rows, go to step 12. If it is more than 10000 rows, go to step 11.

11. Download a MS Excel split tool online and split the file to several smaller files so that the maximum row number does not exceed 10000.

12. Rearrange the data to a table with a script A. The algorithm of script A follows after the end of the present flow chart.

13. Note down the coordinates of points you want to change and use script B to change the data.

14. Select the data of the table and go to conditional formatting→ color scales. Put any color scale on the data so that you can see the terrine. Check if there is any errors or outliers and correct them by hand. 15. Use script C to transverse the table back to columns of data.

16. Copy and paste the changed data to a new MS Excel file and save it as a txt file.

17. In ArcGIS, go to file→ add data→ add xy data and add that text file. Select the correct coordinate system and projection system.

18. Search for ”create TIN” in tool box and use the point data to create TIN

19. Search for ”TIN to Raster” and convert the TIN to a raster file

20. Looping step 4 to 19 until all clips were finished editing

21. Load all clips and the original DEM into ArcGIS and put clips above the original DEM in Table of contents.

22. Go to Windows→ Image Analysis and select all clips and the original DEM.

23. Go to Processing in the Image Analysis window and select first at the Mosaic sub-window

24. Click on mosaic and check the new raster if there is any errors. These errors need to be corrected back in the MS Excel file.

25. Right click on the Mosaic file and go to Data→ Export Data. Define the resolution, format, file name and location then Save.

**Script A**

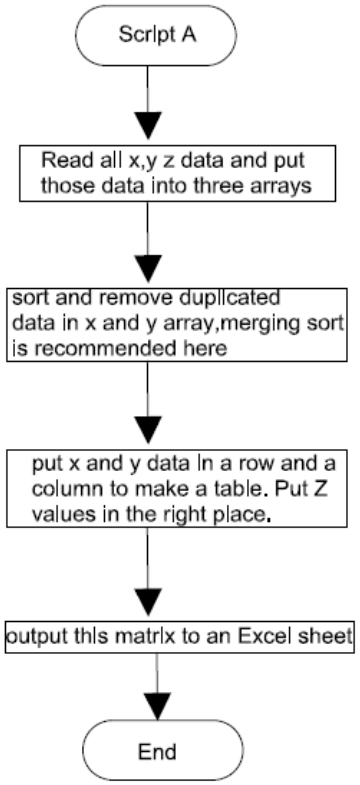


Figure A.2: Script A

1. Count how many rows are there in the data

2. Define 3 vectors with the size of the number of rows of data

3. Read the x,y,z data and put them into three coordinate vector

4. Sort x and y delete the duplicated values, sort again. Merging sort is recommended here because the vector size is usually very big.

5. Define a matrix with column size the number of x and row size the number of y.

6. Read every z values from the z vector and put z value into the right place in the matrix. The pointer of z value in z vector is equal to the pointer in x and y vector. Use the pointers to find the right place in the matrix.

7. Output the matrix to MS Excel.

**Script B**

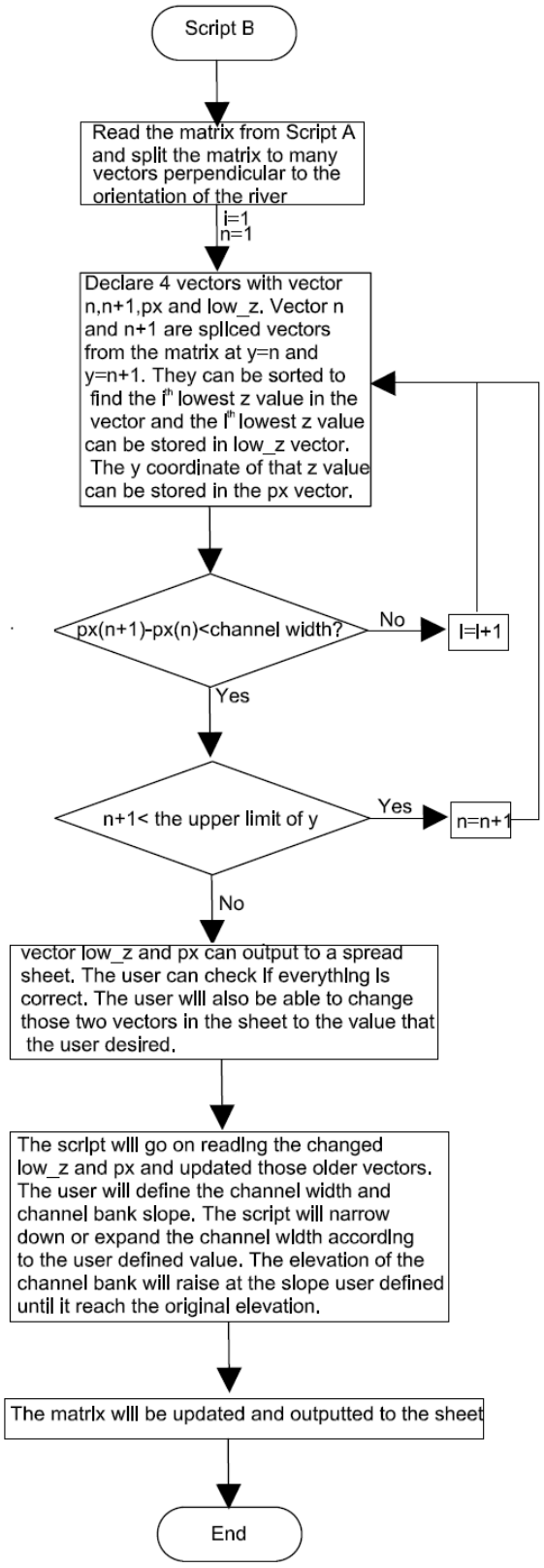


Figure A.3: Script B

The following algorithm treating the river is mostly on y direction. If your river is in x direction, please alternate the coordinate system

1. Read the matrix form Script A and split the matrix according to x coordinates to vectors. There will be a lot of vectors with the z values in it. Each vector has the same x coordinate. Those z values with their x coordinates should form a cross-section of the river.

2. Sort the first vector, find the x coordinate of the smallest z value in the vector and put that x coordinate into a new vector with the size of number of y. This new coordinate vector contains the information of the station of the center of the channel. This vector will be called "x-station" vector in the following steps. Put the smallest z value in this vector to a new vector "channel-height" .

3. Sort the second vector and check if the x coordinate of this vector is in a certain range of the first x. The user needs to define this range. For example, if the first x is 1500, and y coordinates are increasing by 0.5 m, then the second x should not be smaller than 1000 or bigger than 2000 unless the channel is wider than 500 m. That specific range depends on the longitudinal orientation of the channel.

4. Finish sorting all the vectors and give values to the x-station channel-height vectors. Output these vectors to the same MS Excel file with matrix.

5. The user needs to check those two vectors if there is any error. The user can edit those two vectors. The channel-height vector should be the channel profile along y directions. Edit this vector to a user desired channel profile

6. Script B should read the changed x-station vector and channel-height vectors and replace the old values in those vectors.

7. User will define the bottom channel width and channel bank slope. The script will go to the matrix, for every x-station at this y, the z value will be changed to channel-height. Cells in the range of bottom width should also be changed to channel-height. Cells near the border of the range should be changed using z=(channel-height) +slope*(y-range border). This bank height calculation stops at certain condition. For example: At certain y, z was decreased. Then the bank z should use z equation to calculate the new z until the new z is bigger than the original z.

8. Update the matrix and output it to the MS Excel sheet.

**Script C**

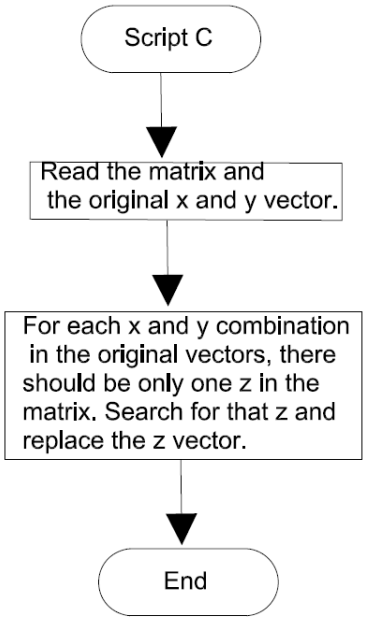


Figure A.4: Script C

1. For each z in the matrix there should be a x and y coordinate. Search this x and y coordinate in the x and y coordinate vector from Script A and change the according z value to the changed value from the matrix.

2. Output the changed x y z vector to a MS Excel sheet